Annu. Rev. Fluid Mech. 2000. 32:1–32

SCALE-INVARIANCE AND TURBULENCE MODELS FOR LARGE-EDDY SIMULATION

Charles Meneveau and Joseph Katz
Department of Mechanical Engineering, Center for Environmental and Applied Fluid Mechanics, The Johns Hopkins University, Baltimore, Maryland 21218; e-mail: meneveau@jhu.edu

Key Words small-scale structure, subgrid-scale modeling

■ **Abstract** Relationships between small and large scales of motion in turbulent flows are of much interest in large-eddy simulation of turbulence, in which small scales are not explicitly resolved and must be modeled. This paper reviews models that are based on scale-invariance properties of high-Reynolds-number turbulence in the inertial range. The review starts with the Smagorinsky model, but the focus is on dynamic and similarity subgrid models and on evaluating how well these models reproduce the true impact of the small scales on large-scale physics and how they perform in numerical simulations. Various criteria to evaluate the model performance are discussed, including the so-called a posteriori and a priori studies based on direct numerical simulation and experimental data. Issues are addressed mainly in the context of canonical, incompressible flows, but extensions to scalar-transport, compressible, and reacting flows are also mentioned. Other recent modeling approaches are briefly introduced.

1. INTRODUCTION

One of the key challenges in turbulence research is to understand relationships between the structure, dynamics, and statistics of small and large scales of motion. Phenomenologically, an important property of turbulence that has received much attention in the past decades is scale invariance. Scale invariance means that certain features of the flow remain the same in different scales of motion. Such a symmetry can be interpreted as a particularly simple relationship between small and large scales and can thus become a useful ingredient in turbulence models.

The idea of scale invariance in turbulence dates back to Richardson (1922), who enunciated it in qualitative terms in his celebrated rhyme, which has been quoted a great many times but is worth repeating here nonetheless:

Big whorls have little whorls,
which feed on their velocity,
and little whorls have lesser whorls,
and so on to viscosity (in the molecular sense).

Quantitatively, when there exists a range of scales (the inertial range) in which effects of viscosity, boundary conditions, and large-scale structures are not important, dimensional analysis (Kolmogorov 1941; for a modern account, see Frisch 1995) leads to the well-known universal power-law spectrum

$$E(k) = c_K \, \varepsilon^{2/3} \, k^{-5/3}. \tag{1}$$

Here c_K is the Kolmogorov constant, k is the wavenumber magnitude, and ε is the dissipation rate of kinetic energy caused by molecular viscosity ν. Equation 1, which is well supported by a large body of experimental data (e.g. see Saddoughi & Veeravalli 1994, Sreenivasan 1995), implies scale invariance in the sense that the quantity $\gamma^{5/3}E(\gamma k)$ remains unchanged in the inertial range under the scale transformation $k \to \gamma k$. Several other features of turbulence have been shown to exhibit scale invariance (Sreenivasan 1991, Sreenivasan & Antonia 1997).

The need for deeper insights into relationships between large and small scales has grown because of the emergence of large-eddy simulation (LES). In LES, one separates the motion into small and large scales by spatially filtering the velocity field with a kernel, $G_\Delta(\mathbf{x})$ (Leonard 1974, Rogallo & Moin 1984, Lesieur & Métais 1996). The convolution kernel, of which the Gaussian filter $G_\Delta^{\text{gaus}}(\mathbf{x}) = [6/(\pi\Delta^2)]^{3/2} \exp(-6x^2/\Delta^2)$, is an example (other filters are discussed in Section 2.2), eliminates scales smaller than Δ. The LES equations are obtained by filtering the Navier-Stokes equations and read

$$\partial_t \tilde{\mathbf{u}} + \tilde{\mathbf{u}} \cdot \nabla \tilde{\mathbf{u}} = -\frac{1}{\rho} \nabla \tilde{p} + \nu \nabla^2 \tilde{\mathbf{u}} - \nabla \cdot \boldsymbol{\tau}^\Delta, \; \nabla \cdot \tilde{\mathbf{u}} = 0, \tag{2}$$

where $\tilde{}$ represents a convolution with $G_\Delta(\mathbf{x})$. Equation 2 is amenable to numerical discretization at a spatial resolution of order Δ, which is typically much more affordable than direct numerical simulation (DNS), which requires resolutions near the Kolmogorov scale, η. Equation 2 includes the divergence of $\boldsymbol{\tau}^\Delta$, the so-called subgrid-scale (SGS) stress tensor:

$$\tau_{ij}^\Delta = \widetilde{u_i u_j} - \tilde{u}_i \tilde{u}_j. \tag{3}$$

To close Equation 2, τ_{ij}^Δ must be expressed in terms of the resolved (filtered) velocity field. To develop SGS models, some guidance has been provided in the past by approaches traditionally used in modeling of the Reynolds stresses. There, spatial features of the mean velocity field, such as its gradients, have been used. Principles of Galilean invariance and realizability have been useful in severely constraining the many expressions that would otherwise be possible (e.g. Speziale 1991). Besides spatial features, history effects can also be taken into account by, for instance, including additional transport equations. In LES, besides the two axes of space and time, the axis of scale emerges. By the very nature of LES, the turbulent velocity fields at scales larger than Δ are available during the simulation. When such scale information is used for SGS modeling, the opportunities for

improvements expand considerably. Concomitant with such new directions, challenges arise that are quite distinct from those typically encountered in Reynolds stress modeling.

The main goal of this article is to examine the current literature on the use of scale information in models for $\boldsymbol{\tau}^{\Delta}$ and to ascertain how well the resulting models reproduce the impact of small-scale turbulence and perform in simulations. Applying the Kolmogorov dimensional analysis to the SGS stress tensor shows that, for Δ in the inertial range, $\boldsymbol{\tau}^{\Delta} \sim \mathbb{C}[(\varepsilon\Delta)^{2/3}]$. This relationship suggests scale invariance; that is, certain features of $\gamma^{-2/3}\boldsymbol{\tau}^{\gamma\Delta}$ remain unchanged under the rescaling $\Delta \rightarrow \gamma\Delta$. Different scale invariance-based models discussed in this article differ in what feature of the stress is assumed to remain unchanged. Differences include whether the invariance holds locally or on average or whether it applies to individual tensor elements or only for certain tensor contractions.

In Section 2 we begin with a brief discussion of how models are evaluated. Section 3 recalls the main features of the traditional Smagorinsky model. Together with a growing set of applications to a variety of flows, the dynamic Smagorinsky model (Germano et al 1991) is reviewed in Section 4. Section 5 addresses the so-called similarity models (Bardina et al 1980, Liu et al 1994) and examines a growing body of literature on their applications. Section 6 continues the discussion initiated in Section 2, providing more details and recent developments on criteria used to evaluate SGS models. Effects of coherent structures, intermittency, and nonequilibrium conditions are discussed in Section 7. Recent new classes of SGS models are summarized in Section 8, and the conclusions are presented in Section 9.

This review concentrates on modeling of the SGS stress. However, for applications of LES, several other issues such as numerical techniques, including the analysis of discretization errors (Ghosal 1996, Kravchenko & Moin 1997), filter inhomogeneity (Ghosal & Moin 1995), and formulations in curvilinear coordinate systems (Jordan 1999), are also crucial. Another current issue concerns the need to model the wall shear stress in simulations of wall-bounded flows that do not explicitly resolve the viscous sublayer (see Mason 1994, Balaras et al 1996). Specification of turbulent inflow (or initial) conditions is also a challenge (Lund et al 1998).

2. STUDYING SUBGRID-SCALE MODELS

2.1 A Posteriori and A Priori Studies

To evaluate the performance of a model for SGS stress [denoted henceforth by $\tau_{ij}^{\Delta,\mathrm{mod}}(\mathbf{x}, t)$], the results from a simulation that uses the model are compared with available data. The data can be from DNS or from experiments, typically in the form of mean velocity and Reynolds stress distributions, spectra, etc. Piomelli et al (1988) coined the name a posteriori tests for such comparisons to emphasize

that the model is evaluated only after it has been implemented in a simulation (see Sections 4 and 5). A posteriori tests are considered to be the ultimate tests of model performance. However, owing to the integrated nature of results (combining effects of numerical discretization, time integration, and averaging), a posteriori tests typically do not provide much insight into the detailed physics of models and the reasons that they do or do not work.

A complementary and perhaps more fundamental approach is based on direct comparison between $\tau_{ij}^{\Delta}(\mathbf{x}, t)$ and $\tau_{ij}^{\Delta,\mathrm{mod}}(\mathbf{x}, t)$. Such a comparison requires data at high spatial resolution that are sufficient to resolve the subgrid-scale range. $\tau_{ij}^{\Delta}(\mathbf{x}, t)$ is evaluated based on its definition (Equation 3), and $\tau_{ij}^{\Delta,\mathrm{mod}}(\mathbf{x}, t)$ is evaluated by processing the filtered data. For such analysis, Piomelli et al (1988) coined the name a-priori test to emphasize that no actual LES is involved. The data for such studies can be generated by using DNS, which allows processing the full three-dimensional velocity field, but is limited to low Reynolds numbers and simple geometries. Clark et al (1979), McMillan & Ferziger (1979), and Bardina et al (1980) are early examples of such studies, and Piomelli et al (1991), Domaradzki et al (1993), and Härtel et al (1994) are more recent examples. An alternative that complements DNS is to use experimental data. This enables the study of high-Reynolds-number flows, but it comes at the cost of providing partial information, because only a subset of all the relevant parameters can be measured. For instance, using planar particle image velocimetry (PIV), two-dimensional distributions of four tensor elements can be measured by means of spatial filtering in two directions (see Liu et al 1994, 1995, for data in the far-field of a round jet; Bastiaans et al 1998 for results in free convection; and Liu et al 1999 for rapidly distorted turbulence). Concentration measurements using laser-induced-flourescence (Dahm et al 1991) have been analyzed to measure the SGS variance of a conserved scalar (Cook & Riley 1994). Using hot-wire single-point sensors, Meneveau (1994), as well as Meneveau & O'Neil (1994), studied grid turbulence, and O'Neil & Meneveau (1997) considered turbulence in a cylinder wake. Porté-Agel et al (1998a) studied turbulence and scalar transport in the atmospheric boundary layer by using a sonic anemometer. These single-point data were analyzed by using temporal filtering, which was interpreted as one-dimensional spatial filtering in the streamwise direction, by invoking the Taylor hypothesis. To achieve quantitatively more accurate results, two-dimensional filtering should be used. It can be approximated by an array of point sensors arranged along a line perpendicular to the mean velocity. This approach has been proposed by Tong et al (1998) and applied by Porté-Agel et al (1999) for sonic anemometer measurements in the atmospheric boundary layer. It has also been applied to hot-wire measurements in laboratory turbulence (Cerutti & Meneveau 1999). The accuracy of two-dimensional filtering and Taylor's hypothesis has been addressed for wall-bounded flows by using DNS (Murray et al 1996) and LES (Tong et al 1998). Finally, techniques for multipoint three-dimensional velocity measurements, e.g. holographic PIV (Barnhart et al 1994, Meng & Hussain 1995, Zhang et al 1997),

are beginning to provide crucial data on the spatial distribution of all the SGS tensor components (Tao et al 1999).

2.2 Separating Between Large and Small Scales

Spatial filtering (Leonard 1974) is the most common approach to conceptually, and in some models operationally, decompose the velocity field into large (resolved) and small (SGS) scales. Pope (2000) presents an exhaustive discussion of various filters and their properties. The most common filters are the spectral cutoff filter $G_\Delta^{\rm sp}(\mathbf{x}) = \Pi_{k=1}^3 \sin(\pi x_k/\Delta)/(\pi x_k)$, the Gaussian filter $G_\Delta^{\rm gaus}(\mathbf{x})$ already introduced in Section 1, and the box or top-hat filter $G_\Delta^{\rm box}(\mathbf{x}) = \Delta^{-3}$ if $|x_k| < \Delta/2$ for all k and $G_\Delta(\mathbf{x}) = 0$ if $|x_k| \geq \Delta/2$. The spectral cutoff filter cleanly separates between scales. However, when filtering spatially localized phenomena, it causes nonlocal oscillatory behavior. Moreover, because $G_\Delta^{\rm sp}$ has negative lobes, the resulting stress tensor does not follow realizability conditions (Vreman et al 1994b) and, for LES of a conserved scalar, the filtered scalar can fall outside allowable bounds. The box filter, on the other hand, has good spatial localization but does not allow unambiguous separation between scales because of spectral overlap. The Gaussian filter has intermediate localization properties in both physical and spectral space, although it is closer to the box filter.

Another method of separating between large and small scales is expanding the velocity field in a set of orthonormal basis-functions and then truncating the summation to define the large-scale field (a projection). The discarded modes represent the SGS range. For Fourier modes, this method is equivalent to a spectral cutoff filter. For other basis functions that are spatially more compact such as wavelets (e.g. see Meneveau 1991), or for POD eigenfunctions (e.g. see Berkooz et al 1993), the task of deriving the equations for the resolved field is more complicated than with homogeneous spatial filters. Hence, to date these directions have not been much pursued for LES. Recently, Farge et al (1999) have proposed an interesting separation into non-Gaussian resolved, and Gaussian unresolved, motions in two-dimensional turbulence.

2.3 Comparisons Between Real and Modeled Stresses

Once the data are processed to generate signals or fields of measured $\boldsymbol{\tau}^\Delta(\mathbf{x}, t)$ and $\boldsymbol{\tau}^{\Delta,\rm mod}(\mathbf{x}, t)$, one must decide how precisely they should be compared. Contrary to the traditional Reynolds stress tensor, $\boldsymbol{\tau}^\Delta(\mathbf{x}, t)$ and $\boldsymbol{\tau}^{\Delta,\rm mod}(\mathbf{x}, t)$ are fluctuating stochastic variables. Figure 1*a* is a representative field of $\tau_{12}^\Delta(\mathbf{x}, t)$ (Liu et al 1994) demonstrating a high degree of spatial variability. An integrated figure of merit of the local agreement between real and modeled stresses within realizations of the flow has often been given in terms of their correlation coefficient $\rho(\boldsymbol{\tau}^\Delta, \boldsymbol{\tau}^{\Delta,\rm mod})$ (Clark et al 1979); representative results are presented in Sections 3 and 5. Very often, however, one is not interested in so much detail, but only in the ability of LES to generate the correct flow statistics, such as distributions of mean and rms

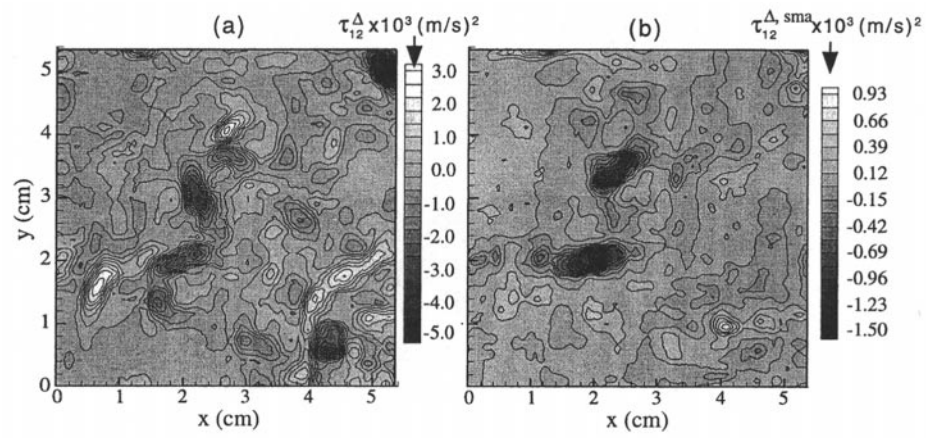

Figure 1 Contour plots of subgrid-scale (SGS) shear stress distribution in the far-field of a round turbulent jet measured by using particle image velocimetry. (*a*) The experimental SGS stress; (*b*) the prediction of the Smagorinsky model with $c_s = 0.1$ (replotted from Liu et al 1994).

velocities, spectra, etc. It is often argued that the most important statistical feature of $\boldsymbol{\tau}^{\Delta}$ is how it affects the mean dissipation of kinetic energy (for supporting arguments, see Section 6). The mean resolved kinetic energy $\mathcal{K}$ (Piomelli et al 1991) evolves according to

$$\frac{\partial \mathcal{K}}{\partial t} + \langle \tilde{u}_j \rangle \frac{\partial \mathcal{K}}{\partial x_j} = -\frac{\partial A_j}{\partial x_j} - 2\nu \langle \bar{S}_{ij} \bar{S}_{ij} \rangle - \Pi^{\Delta} + \langle \tilde{f}_i \tilde{u}_i \rangle. \quad (4)$$

Here $\mathcal{K} = \frac{1}{2} \langle \tilde{u}_i \tilde{u}_i \rangle$, and the brackets denote ensemble averaging. A_j is a flux term consisting of resolved velocity third-order moments, as well as pressure, SGS stress, and viscous stress transport. The second term on the right hand side is dissipation of resolved energy due to molecular viscosity. This term is negligible for large Δ/η and high Reynolds numbers. The last term is energy injection by body forces. In the inertial range, the most important effect of the unresolved scales on the evolution of $\mathcal{K}$ is $\Pi^{\Delta} \equiv -\langle \tau_{ij}^{\Delta} \tilde{S}_{ij} \rangle$, the so-called SGS dissipation of kinetic energy. Typically Π^{Δ} acts as a sink of resolved kinetic energy. It also appears as a source term for SGS kinetic energy $\frac{1}{2} \tau_{ii}^{\Delta}$. In fact, $\Pi^{\Delta} = \varepsilon$ when the SGS kinetic energy is assumed to be in equilibrium and Δ is in the inertial range (Lilly 1967). Equation 4 indicates that a model must faithfully reproduce Π^{Δ} so that the LES computes the correct evolution of $\mathcal{K}$. However, as discussed in Section 6, providing the correct mean dissipation is in general only a necessary but not a sufficient condition to reproduce the correct flow statistics.

Given the special importance of SGS energy dissipation, it has been the focus of a number of studies. For instance, Piomelli et al (1991) study the details of $-\tau_{ij}^{\Delta} \tilde{S}_{ij}$ and its average in DNS of plane channel flow. Before averaging, a sig-

nificant portion of the flow exhibits backscatter, that is, negative values of $-\tau_{ij}^{\Delta}\tilde{S}_{ij}$ in which energy is transferred from SGS to resolved scales. The mean, Π^{Δ}, however, is found to be positive. A priori studies of the SGS energy dissipation in isotropic turbulence have shown that most of the energy that is transferred to the SGS range below Δ originates from the octave above, that is, from scales between Δ and 2Δ (Domaradzki et al 1993).

3. SMAGORINSKY MODEL

The Smagorinsky model (Smagorinsky 1963, Lilly 1967) for the deviatoric part of the stress, $\tau_{ij}^{\Delta} - \frac{1}{3}\tau_{kk}^{\Delta}\delta_{ij}$, is defined as

$$\tau_{ij}^{\Delta,\mathrm{smag}} = -2\nu_T\tilde{S}_{ij}, \tag{5}$$

where ν_T is the (scalar) eddy viscosity and $\tilde{S}_{ij} = \frac{1}{2}(\partial_j\tilde{u}_i + \partial_i\tilde{u}_j)$ is the resolved strain-rate tensor. ν_T is constructed as the product of a length scale ($\sim\Delta$) and a velocity difference at that scale [$\sim\Delta|\tilde{S}|$, where $|\tilde{S}| \equiv (2\tilde{S}_{ij}\tilde{S}_{ij})^{1/2}$]. Thus

$$\nu_T = (c_s^{\Delta}\Delta)^2|\tilde{S}|, \tag{6}$$

where c_s^{Δ} is the Smagorinsky coefficient which, in principle, may depend on scale. The Smagorinsky model has been described previously by Moin & Kim (1982), Rogallo & Moin (1984), Lesieur & Métais (1996), and in depth by Pope (2000).

A comparison between $\tau_{12}^{\Delta,\mathrm{smag}}$, shown in Figure 1*b*, and the real distribution, shown in Figure 1*a*, exhibits significant differences. This deficiency of eddy viscosity models was originally observed from DNS data by Clark et al (1979), McMillan & Ferziger (1980), and Bardina et al (1980). Quantitatively, the correlation coefficient $\rho(\boldsymbol{\tau}^{\Delta}, \boldsymbol{\tau}^{\Delta,\mathrm{smag}})$ typically ranges from 0 to $\sim$0.25 (Clark et al 1979, Liu et al 1994). The correlations are slightly larger ($\rho \sim 0.4$) when the SGS force $\nabla\cdot\boldsymbol{\tau}^{\Delta}$ is compared with $\nabla\cdot\boldsymbol{\tau}^{\Delta,\mathrm{smag}}$. Typically the correlation is still higher ($\rho \sim 0.5$–0.7) when comparing the local SGS dissipation rate $-\tau_{ij}^{\Delta}\tilde{S}_{ij}$ with $-\tau_{ij}^{\Delta,\mathrm{smag}}\tilde{S}_{ij}$ (Clark et al 1979).

The foregoing comparisons imply that, for an individual realization of the flow, the eddy viscosity model does not adequately capture the proper physics of SGS turbulence. This behavior is in contrast to molecular viscosity. For instance, a priori testing to study the viscous stress tensor in the context of the kinetic theory of gases would consist of measuring all of the molecules' instantaneous fluctuating velocities, computing the stress tensor by averaging inside a small control volume, and comparing with the imposed macroscopic shear. If the control volume is large compared with the mean free path and the macroscopic shear is low compared with the inverse collision times, the relationship between the stress and shear should be (nearly) deterministic and linear (Landau & Lifshitz, 1980). In turbulence, there is no such separation of length and time scales. Therefore, it is

not surprising that comparisons of $\tau_{ij}^{\Delta}(\mathbf{x}, t)$ with $\tilde{S}_{ij}$ yield poor results. This problem is a familiar one in the context of Reynolds stresses (see e.g. Speziale 1991), where it occurs at the largest scales of turbulence. None of the several variants of the eddy viscosity model (see Sections 3.1 and 4) is exempt from this fundamental problem.

As discussed in Section 2, the Smagorinsky model can also be tested a priori by comparing mean SGS dissipation, that is, comparing $-\langle \tau_{ij}^{\Delta} \tilde{S}_{ij} \rangle = \Pi^{\Delta}$ with $-\langle \tau_{ij}^{\Delta,\mathrm{smag}} \tilde{S}_{ij} \rangle$. For homogeneous turbulence, c_s^{Δ} can be adjusted to enforce that $\langle \tau_{ij}^{\Delta} \tilde{S}_{ij} \rangle = \langle \tau_{ij}^{\Delta,\mathrm{smag}} \tilde{S}_{ij} \rangle$. This procedure was first used by Lilly (1967) in his landmark paper, for isotropic turbulence with Δ in the inertial range. Equation 4 for statistically stationary isotropic turbulence with $\Delta \gg \eta$ yields $\langle f_i \tilde{u}_i \rangle = \Pi^{\Delta}$. Using the equilibrium assumption $\Pi^{\Delta} = \varepsilon$ and replacing τ_{ij}^{Δ} with the Smagorinsky model, one obtains

$$\varepsilon = 2^{3/2} (c_s^{\Delta} \Delta)^2 \langle (\tilde{S}_{ij} \tilde{S}_{ij})^{3/2} \rangle \tag{7}$$

as a necessary condition for the model to reproduce the correct energetics of the resolved scales. With the approximation $\langle |\bar{S}|^3 \rangle \simeq \langle |\bar{S}|^2 \rangle^{3/2}$, a Kolmogorov spectrum (Equation 1), and a spectral cutoff filter to evaluate $\langle |\bar{S}|^2 \rangle$, Lilly's (1967) classical result $c_s^{\Delta} = \pi^{-1}(2/3c_K)^{4/3} \approx 0.16$ (for $c_K = 1.6$) is obtained. The coefficient is thus scale-invariant in the inertial range. When dealing with grids of unequal sizes in each direction (e.g. $\Delta_1 < \Delta_2 < \Delta_3$), the above derivation can be repeated by using an anisotropic three-dimensional filter (Scotti et al 1993). To zero order in $\log(a_i)$ (where $a_1 = \Delta_1/\Delta_3$ and $a_2 = \Delta_2/\Delta_3$ are the two grid aspect ratios), the analysis yields that Δ in the definition of ν_T must be replaced with a length-scale based on the cell volume, $\Delta_{\mathrm{eq}} = (\Delta_1 \Delta_2 \Delta_3)^{1/3}$. This expression is equal (and thus serves as a formal justification) to the empirical length scale originally proposed by Deardorff (1974). For very large filter anisotropies, Scotti et al (1993) show that, in addition to the use of Δ_{eq}, c_s^{Δ} should be replaced with $c_s^{\Delta} f(a_1, a_2)$, where $f(a_1, a_2) \approx \cosh\{(4/27)[(\ln a_1)^2 - \ln a_1 \ln a_2 + (\ln a_2)^2]\}^{1/2}$.

3.1 Other Eddy Viscosity Models

There are many variants of the Smagorinsky model that differ mainly in how the eddy viscosity is defined. One variant is the so-called kinetic energy model (Schumann 1975), in which $\nu_T = C_e e^{1/2} \Delta$ and $e = \frac{1}{2} \tau_{ii}^{\Delta}$. An additional scalar transport equation for e is solved, in which diffusion and dissipation terms must be modeled. This approach incorporates memory effects and has been popular in simulations of atmospheric flows (Moeng 1984, Shaw & Schumann 1992, Mason 1994).

Kraichnan (1976) used two-point closures to show that, if one considers in detail how the eddy viscosity acts upon different wavenumber modes, the eddy viscosity must be allowed to depend on the wavenumber magnitude based on a function $\nu_T(k, k_c)$ (the spectral eddy viscosity), where $k_c = \pi/\Delta$. For the spectral cutoff filter, the closures predict that $\nu_T(k, k_c)$ has a cusp near k_c (Kraichnan 1976,

Leslie & Quarini 1979, Chasnov 1991). This prediction has been verified in DNS (Domaradzki et al 1987) and has been used in pseudospectral LES. As reviewed in Lesieur & Métais (1996), the cusp behavior is simple to implement in such simulations, but it is more involved to implement in physical space for inhomogeneous flows. A possible approach is to use higher-order Laplacians or hyperviscosity terms (e.g. see Dantinne et al 1998). Details about the SGS turbulence can also be incorporated by solving model equations of $E(k, t)$, for $k \geq k_c$. An interesting initial attempt in this direction coupling LES with an explicit model of $E(k, t)$ based on the eddy-damped quasi normal approximation (EDQNM) is described in Chollet & Lesieur (1981).

An alternative to the Smagorinsky model is the so-called structure function model (Métais & Lesieur 1992). The eddy viscosity is expressed in terms of a physical-space estimate of the energy spectral density near k_c. A number of variants of this model that involve various secondary filtering operations, along with a number of applications, are described in Lesieur & Métais (1996). Eddy viscosity SGS models have also been studied with renormalization group techniques (Yakhot et al 1989, Smith & Woodruff 1998).

3.2 Limitations

As mentioned in Section 2.3, measurements of the local SGS dissipation, $-\tau_{ij}^{\Delta}\tilde{S}_{ij}$, often exhibit regions in which the dissipation is negative (Piomelli et al 1991, Liu et al 1994). In contrast, the eddy viscosity model is always purely dissipative, that is, $-\tau_{ij}^{\Delta,\mathrm{smag}}\tilde{S}_{ij} \geq 0$. It assumes erroneously that the eigenvectors of the tensor $\tau_{ij}^{\Delta} - \frac{1}{3}\tau_{kk}^{\Delta}\delta_{ij}$ are aligned with those of $\tilde{S}_{ij}$.

The Smagorinsky model also has limitations in terms of mean quantities, such as mean SGS dissipation, when the grid scale approaches the limits of the inertial range. For instance, when the resolved flow is laminar, the standard value of c_s overestimates the SGS stress and dissipation, often preventing transition to turbulence (Piomelli & Zang 1991). A similar problem exists in the viscous sublayer, where τ_{12}^{Δ} must drop to 0 at the wall as x_2^3 (x_2 is the wall-normal coordinate). Conversely, $\tau_{12}^{\Delta,\mathrm{smag}}$ with a fixed coefficient remains finite owing to the mean shear. The model is thus too dissipative and in the past has required empirical wall-damping functions. Such functions are also needed in LES of high-Reynolds-number flows over smooth or rough walls, when one cannot afford to resolve the viscous sublayer (Mason 1994). In those cases the first grid point falls in the log layer (if it exists), and the grid scale is comparable to the distance to the wall, that is, the local integral scale. In the other limit ($\Delta \to \eta$), the coefficient must vary with Δ even in isotropic turbulence, to reproduce the correct SGS dissipation rate in the viscous range (Voke 1996, Meneveau & Lund 1997, Pope 2000). The presence of stratification, shear, or rotation also affects SGS dissipation in such a way that a constant scale-invariant coefficient is inappropriate (see Canuto & Cheng 1997). The same is true when turbulence is rapidly distorted away from

equilibrium conditions by, e.g., rapid straining (McMillan et al 1980, Liu et al 1999, Piomelli et al 1997). In general, then, to faithfully reproduce SGS dissipation, c_s cannot be assumed to be flow and situation independent unless Δ is contained well inside an ideal inertial range of locally isotropic and homogeneous turbulence.

Besides SGS dissipation, when the grid scale approaches the integral scale ($\Delta \to \ell$), the mean SGS stress $\langle \tau_{ij}^{\Delta} \rangle$ can contribute significantly to the mean momentum transport (the ensemble average of Equation 2). It is typically quite difficult for the eddy viscosity model to reproduce the correct distributions of both mean energy dissipation and mean stresses (see e.g. Bastiaans et al 1998). In spite of these fundamental drawbacks, the Smagorinsky model has been popular in many applications owing to its simplicity, numerical robustness, and lack of numerical instabilities. However, it often leads to inaccurate results (see Section 5.3).

4. THE DYNAMIC MODEL

The dynamic model (Germano et al 1991) consists of using the resolved scales to measure the model coefficient during the simulation, thus avoiding the need to prescribe or tune the coefficient. The approach uses the assumption of scale invariance by applying the coefficient measured from the resolved scales to the SGS range. Formally, the dynamic procedure is based on the Germano identity (Germano 1992)

$$L_{ij}(\mathbf{x}, t) = \tau_{ij}^{\alpha\Delta}(\mathbf{x}, t) - \overline{\tau_{ij}^{\Delta}(\mathbf{x}, t)}, \text{ where} \tag{8}$$

$$L_{ij} = \overline{\tilde{u}_i \tilde{u}_j} - \overline{\tilde{u}_i}\,\overline{\tilde{u}_j} \tag{9}$$

is the resolved stress tensor, and an overline $\overline{(\ )}$ denotes test filtering at a scale $\alpha\Delta$. This identity can be used to determine unknown model coefficients during the simulation. For this purpose, modeling approximations for τ_{ij}^{Δ} and $\tau_{ij}^{\alpha\Delta}$ are replaced in Equation 8. For the Smagorinsky model one obtains

$$L_{ij} - \frac{1}{3} L_{kk}\delta_{ij} = (c_s^{\Delta})^2 M_{ij}, \text{ where} \tag{10}$$

$$M_{ij} = -2\,\Delta^2 \left[\alpha^2 \left(\frac{c_s^{\alpha\Delta}}{c_s^{\Delta}} \right)^2 \overline{|\tilde{S}|}\;\overline{\tilde{S}}_{ij} - \overline{|\tilde{S}|\;\tilde{S}_{ij}} \right]. \tag{11}$$

It has been assumed that c_s^{Δ} is spatially uniform to justify extracting it from under the test-filtering operation (Ghosal et al 1995). From here on we follow the most common choice of $\alpha = 2$. Explicit assumption of scale invariance, i.e. $c_s^{2\Delta} = c_s^{\Delta}$, allows M_{ij} to be fully determined from the resolved motions during LES.

Because Equation 10 should hold at every point and time and for five inde-

pendent tensor elements (M_{ij} is trace free in incompressible flow), it is an overdetermined system that a single c_s^Δ cannot satisfy exactly. Because the Smagorinsky model does not reproduce the details of the stresses (regardless of the value of c_s^Δ), Equation 10 must be understood to hold, at best, in an average sense only. The various formulations of the dynamic model differ on how this condition is enforced. Originally, Germano et al (1991) have contracted Equation 10 with $\tilde{S}_{ij}$. One obtains $(c_s^\Delta)^2 = \langle L_{ij}\tilde{S}_{ij}\rangle / \langle M_{ij}\tilde{S}_{ij}\rangle$. A subsequent and more widespread approach (Lilly 1992) is based on minimizing the square error, $\mathscr{E} = \langle [L_{ij} - (c_s^\Delta)^2 M_{ij}]^2 \rangle$ and leads to

$$(c_s^\Delta)^2 = \frac{\langle L_{ij} M_{ij}\rangle}{\langle M_{ij} M_{ij}\rangle}. \tag{12}$$

Without the averaging, the dynamic model has been found to yield a highly variable eddy viscosity field (e.g. see Liu et al 1995) including significant portions with negative values, which is destabilizing in numerical simulations. Highly variable coefficients also complicate deriving Equation 10 from Equation 8, because c_s^Δ depends on location and cannot simply be extracted from the test-filter operation (for an in-depth discussion and a rigorous, but somewhat involved, remedy, see Ghosal et al 1995, Piomelli & Liu 1995). The procedure of averaging over directions of statistical homogeneity used by Germano et al (1991) circumvents these problems. It has been given a formal basis by Ghosal et al (1995), who show that this procedure minimizes the total error in the homogeneous region over which the averaging is performed. Using this approach, Piomelli (1993) has obtained accurate results in channel flow by averaging the equations over planes parallel to the walls. Figure 2 shows that the resulting dynamic coefficient (multiplied by the x_2–dependent grid-scale Δ) displays the correct x_2^3 behavior near the wall.

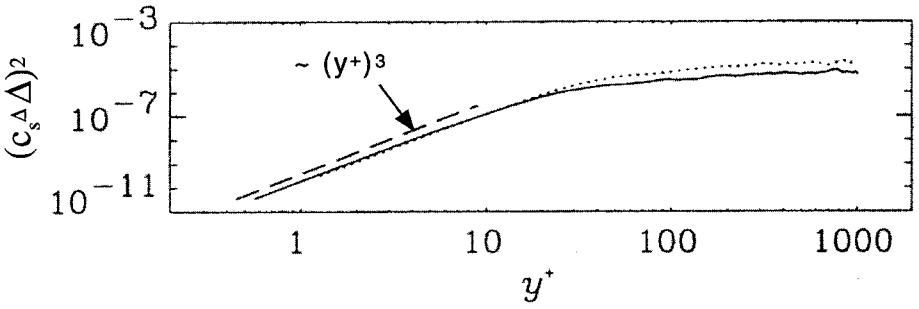

Figure 2 Near-wall scaling of the dynamic coefficient in channel flow at $R_\tau = 1050$. Solid and dotted lines are results using different resolutions. The dashed line represents a x_2^{+3} slope (from Piomelli 1993, Figure 8a).

The dynamic Smagorinsky model has since been applied to many flows, generally with good results. As examples, we mention LES of rotating channel flow (Piomelli & Liu 1995), mixing layers (Ghosal & Rogers 1997), scalar mixing in coannular jets (Akselvoll & Moin 1996), and a two-dimensional turbulent boundary layer over a bump (Wu & Squires 1997). Results from a workshop on LES of flow around bluff bodies can be found in Rodi et al (1997). They report that the dynamic model predicts the distributions of eddy viscosity better than the traditional Smagorinsky model, but this improvement does not necessarily lead to better flow predictions mainly owing to numerical issues.

Piomelli et al (1988) provide an early discussion of the consistency between numerical techniques, filter type, and SGS models. Analyses of the effects of numerical methods (such as discretization) on the dynamic model have so far been somewhat inconclusive. Most successful tests typically use spectral methods and cutoff filtering in homogeneous directions. Problems with finite-difference implementations of the dynamic model in channel flow have been pointed out (Lund & Kaltenbach 1995), but good results were obtained by Balaras et al (1995). Lund & Kaltenbach (1995) propose prefiltering of the velocity before evaluating model coefficients to avoid inclusion of the smallest resolved scales, which are those most contaminated by numerical errors. Najjar & Tafti (1996), on the other hand, argue that the dynamic model has the ability to adjust appropriately to details of the numerical discretization. In Scotti et al (1997) the dynamic model is found to automatically reproduce the main trends of the correction function, $f(a_1, a_2)$ of Section 3, for high aspect-ratio, pancake-type grids. However, for pencil-type grids (i.e. two directions are better resolved and only one is coarse), the dynamic model leads to considerable underprediction of the coefficient. Clearly, our understanding of the interplay between numerical and modeling issues is presently quite limited.

4.1 Averaging in Complex Geometries

Difficulties in applying Equation 12 arise in flows that do not possess directions of statistical homogeneity. Carati et al (1996) propose ensemble averaging of many simultaneous computations that do not require homogeneous directions. A disadvantage is that random meandering of large-scale structures from one realization to another inevitably leads to spatial smearing of the coefficient field.

Another option is time averaging. To comply with Galilean invariance, time averaging should be formulated in a Lagrangian frame of reference. The Lagrangian dynamic model (Meneveau et al 1996) accumulates the required averages over flow pathlines by backwards time integration, with a weighting function that gives decreasing weights to past events. An exponential weighting function allows one to write the required averages as the solutions to a pair of forward relaxation-transport equations. The chosen relaxation time scale increases when $L_{ij}\mathrm{M}_{ij} < 0$ to prevent the coefficient from becoming negative. This formulation has been applied successfully to forced and decaying isotropic turbulence and in fully

developed and transitional channel flow (Meneveau et al 1996), in particle-laden flows (Wang & Squires 1996), in reacting flows (Réveillon & Vervisch 1996), in nonequilibrium flows (Sarghini et al 1999; see also Section 5.3), and in simulations on unstructured deforming meshes (Haworth & Jansen 1999). Owing to the relatively short time scale, the model is capable of responding quickly to unsteadiness in the mean flow. The sensitivity to a prescribed time scale parameter has been found to be small.

4.2 Generalizations

The relationship between different scales embodied in the Germano identity has been used in other models and evolution equations. As an alternative to the Smagorinsky model, in the so-called Kolmogorov model (Carati et al 1995b), the eddy viscosity is expressed in terms of its inertial-range scaling $\nu_T = C\varepsilon^{1/3}\Delta^{4/3}$. The dimensional quantity $C\varepsilon^{1/3}$ is assumed to be scale invariant and is determined from the dynamic procedure. To model backscatter of kinetic energy from small to large scales, a random force can be added to the eddy-viscosity model (Leith 1990, Chasnov 1991, Mason & Thomson 1992, Schumann 1995). An attempt to obtain the backscatter model coefficient dynamically is described in Carati et al (1995a).

For LES involving transport of scalars such as temperature or concentration, the SGS Prandtl number can be obtained dynamically (Moin et al 1991). This reference also treats compressible turbulence, in which a model is also required for the trace of the SGS stress (because $\tilde{p}$ and not the combination $\tilde{p} + \rho\tau_{ii}^{\Delta}$ is required in the equation of state). Using as base model $\tau_{ii}^{\Delta} = C_I\Delta^2|\tilde{S}|^2$, C_I can be determined from the Germano identity. Réveillon & Vervisch (1996) have successfully applied this model by using the Lagrangian averaging approach. The dynamic approach has also been used successfully to evaluate the two model coefficients for the unclosed diffusion and dissipation terms appearing in the kinetic energy equation (Ghosal et al 1995, Menon et al 1996). Moreover, a dynamic eddy diffusion model for the vorticity transport equation has been developed (Mansfield et al 1998) and applied to Lagrangian vorticity-based LES of colliding vortex rings (Mansfield et al 1999).

In reacting flows, other parameters must be prescribed, providing additional possibilities to apply the dynamic procedure. So-called pdf methods (Pope 1985, Colucci et al 1998) require solving a transport equation for the scalar probability-density function (pdf), which allows one to evaluate the reaction term exactly. A generalization of the pdf method to LES, discussed in Pope (1990) and Gao & O'Brien (1993) requires modeling of the diffusion of the large-eddy pdf. Gao & O'Brien (1993) propose to apply the dynamic model to solve for the unknown eddy diffusion coefficient. DesJardin & Frankel (1998) have applied the dynamic model to close SGS enthalpy-velocity and SGS velocity-kinetic energy correlations required in the mixture fraction and thermal-energy equations. Im et al (1997) use the dynamic approach to close the G-equation for tracking flamelet propagation.

Another possible use of the Germano identity consists of evaluating the error $\mathscr{E}$ during a simulation (Meneveau & Katz 1999a). This procedure estimates the SGS model's accuracy in reproducing the flow features at scales between the grid and test filters and could potentially be used to compare different models during LES [see Anderson & Meneveau (1999)].

4.3 Breaking of Scale Invariance

As discussed in Section 3.2, scale invariance near the grid filter scale Δ does not always hold. In Meneveau & Lund (1997), the standard dynamic model, which assumes $c_s^{2\Delta} = c_s^{\Delta}$, is applied to forced isotropic turbulence across the transition from LES to DNS ($\Delta \to \eta$). The dynamic coefficient decreases with decreasing Δ/η, in agreement with results from a priori tests. However, the results are incorrect quantitatively.

The coefficient also depends on scale when $\Delta \to \ell$. In this limit, Porté-Agel et al (1998b) examine the dynamic model in LES of wall-bounded flows in which the viscous sublayer is not resolved. To account for dependence on Δ, they propose a scale-dependent dynamic model that makes the much weaker assumption of power-law behavior ($c_s^{\alpha\Delta} = c_s^{\Delta}\alpha^{\phi}$ with $\phi \neq 0$). Two Germano identities are written for two different test-filter ratios (e.g. $\alpha_1 = 2$, $\alpha_2 = 4$), providing two equations for two unknowns: c_s^{Δ} and ϕ. Thus, the dynamic procedure is used to learn how the coefficient varies with Δ from the resolved scales, improving the accuracy of the extrapolation to smaller scales. Evidently, the dynamic procedure offers the opportunity for many further generalizations.

5. THE SIMILARITY MODEL

In the similarity model, first introduced by Bardina et al (1980), the assumption of scale invariance is used in a strong and almost literal sense. Here the full structure of the velocity field at scales below Δ is postulated to be similar to that at scales above Δ. This postulate has been given an empirical basis from band-pass–filtered PIV measurements (Liu et al 1994). In that paper, vector maps from successive bands of scales show that certain structures occur simultaneously at different scales at nearly the same locations. Consequently, it is suggested that τ_{ij}^{Δ} must also be similar to a stress tensor constructed from the resolved velocity field,

$$\tau_{ij}^{\Delta,\mathrm{sim}} = C_{\mathrm{sim}}\,(\overline{\tilde{u}_i\tilde{u}_j} - \overline{\tilde{u}}_i\overline{\tilde{u}}_j). \tag{13}$$

Here again an overline represents a second filter, now at some scale $\gamma\Delta$ with $\gamma \geq 1$. As an illustration, Figure 3*a*, which shows $\tau_{12}^{\Delta,\mathrm{sim}}$ determined using the same data as in Figure 1, agrees much better with τ_{12}^{Δ} of Figure 1*a* than $\tau_{12}^{\Delta,\mathrm{smag}}$ does. Many different forms of the similarity model exist. Although they differ in details (e.g. the value of C_{sim} and γ), they have common basic characteristics and trends.

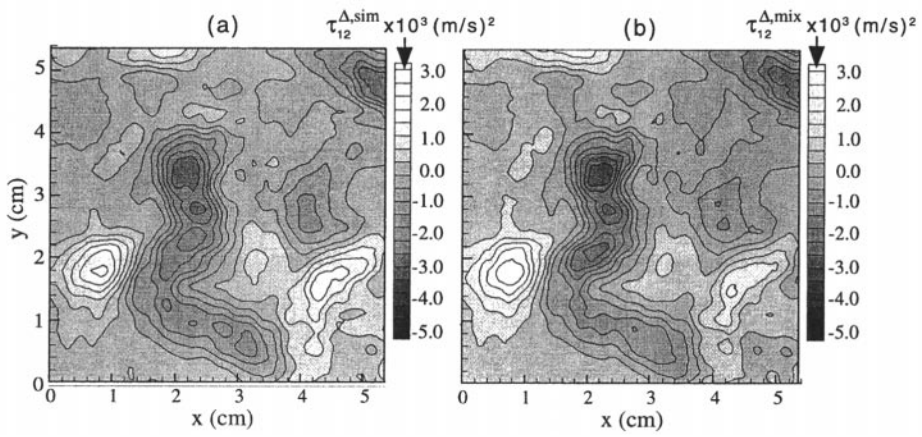

Figure 3 Modeled subgrid-scale shear stress distribution in the far-field of a round turbulent jet (replotted from Liu et al 1994). (*a*) Similarity model with $\gamma = 2$ and $Csim = 1$, (*b*) mixed model with $cs = 0.08$, $\gamma = 2$, and $Csim = 0.9$ (see Meneveau & Katz 1999a). Both use the same data as Figure 1.

Below we summarize the various versions without ascribing great significance to the differences. The original Bardina model uses $\gamma = 1$. Liu et al (1994) propose $\gamma = 2$, whereas Akhavan et al (1999) use $\gamma = 4/3$. There are also differences in whether the trace of $\tau_{ij}^{\Delta,\text{sim}}$ is subtracted or not and also in the type of secondary filtering. Choices for the most appropriate filter and its relationship with the numerical method are, as yet, unresolved matters.

The a priori tests of Bardina et al (1980) performed with Gaussian or box filters show high correlations between real and modeled stresses, typically as high as 80% (although lower for the SGS force and dissipation). Another realistic feature of the similarity model is that it produces backscatter of energy. However, when implemented in simulations, the similarity model alone does not dissipate enough energy and typically leads to inaccurate results. Faced with this difficulty, Bardina et al (1980) suggest adding a dissipative Smagorinsky term. The resulting mixed model is

$$\tau_{ij}^{\Delta,\text{mix}} = C_{\text{sim}} \left(\overline{\tilde{u}_i \tilde{u}_j} - \overline{\tilde{u}}_i \overline{\tilde{u}}_j\right) - 2 \left(c_s^{\Delta}\Delta\right)^2 |\tilde{S}| \, \tilde{S}_{ij}. \tag{14}$$

This mixed model combines the strengths of both the similarity and the Smagorinsky models. Typically the magnitude of the similarity term is significantly higher than that of the Smagorinsky term. Hence, the eddy viscosity term does not degrade the high correlation coefficient (Liu et al 1995). Figure 3*b* shows that the stress distribution for the mixed model barely differs from the similarity model.

In simulations of recirculating flows, Zang et al (1993) implement, with good results, a dynamic mixed model with $\gamma = 1$, $C_{\text{sim}} = 1$, and c_s^{Δ} determined dynamically (in addition to SGS dissipation, some numerical dissipation occurs owing

to the upwinding in their code). Wu & Squires (1998) have successfully applied the dynamic mixed model with Lagrangian averaging in simulations of three-dimensional boundary layers.

The value of $C_{\rm sim}$ depends on the details of implementation and on the filter. In early papers, $C_{\rm sim} = 1$ has been chosen based on Galilean-invariance arguments (Speziale 1985). However, with the currently standard definition of Equation 13 which is already Galilean invariant (see Germano 1986), no such limitation exists. Still, Liu et al (1995) find values close to $C_{\rm sim} \approx 1$ from a priori tests requiring a correct SGS dissipation rate. Cook's (1997) analytical results for a Kolmogorov spectrum with large- and small-scale cutoffs also yield $C_{\rm sim} \sim \mathcal{O}(1)$ (but with variations as the limits of the inertial range are approached). This analysis is based on the condition that $\langle \tau_{ii}^{\Delta} \rangle = \langle \tau_{ii}^{\Delta,{\rm sim}} \rangle$.

Instead of specifying $C_{\rm sim}$, it can be obtained from the dynamic procedure. A two-parameter dynamic mixed model in which both c_s and $C_{\rm sim}$ are determined dynamically has been proposed by Vreman et al (1994a) for $\gamma = 1$ and analyzed for $\gamma = 2$ in Liu et al (1995). These coefficients are found by minimizing the error in the Germano identity leading to a 2×2 system of equations. Another version has been proposed and tested by Salvetti & Banerjee (1995). It includes an ad hoc modification in the similarity part, which simplifies its implementation. Horiuti (1997) has proposed another version as discussed in Section 5.3.

Generalizations of the similarity model to compressible flows are described in Erlebacher et al (1992) (a nondynamic version), as well as in Vreman et al (1995) and Salvetti & Banerjee (1995) (dynamic versions). Based on analysis of experimental data, the similarity model has also been used for modeling the SGS scalar variance (Cook & Riley 1994) needed in presumed-pdf combustion models. Other recent applications of the similarity model to combustion can be found in Desjardin & Frankel (1998) and Jaberi & James (1998).

5.1 The Nonlinear or Gradient Model

Implementation of the mixed model involves additional computational expense owing to the secondary filterings. The latter can be avoided by expanding $\tilde{\mathbf{u}}$ in a Taylor series and performing the filtering analytically (Leonard 1974, Clark et al 1979, Liu et al 1994). The result has the form of a nonlinear, gradient, or tensor eddy viscosity model,

$$C_{\rm sim}\,(\overline{\tilde{u}_i\tilde{u}_j} - \overline{\tilde{u}}_i\overline{\tilde{u}}_j) \cong C_{\rm nl}\,\Delta^2\,\frac{\partial \tilde{u}_i}{\partial x_k}\,\frac{\partial \tilde{u}_j}{\partial x_k}, \qquad (15)$$

where $C_{\rm nl}$ depends on γ and filter type. Equation 15 is applicable only to filters with finite second moments (i.e. it is not applicable to the cutoff filter). Problems occur near walls where the nonlinear model does not follow the required x_2^3 behavior (Liu et al 1994). A detailed a priori analysis of the nonlinear model based on Gaussian-filtered DNS of isotropic turbulence can be found in Borue & Orszag (1998).

Another justification for such a nonlinear model has been pointed out by Leonard (1997) and Winckelmans et al (1998). For a Gaussian filter, given the filtered velocity field without truncation to a discrete grid, one could recover the full velocity field by defiltering. A first-order approximation of τ_{ij}^{Δ} computed from such a defiltered field is equal to the nonlinear model (Equation 15) with $C_{\rm nl} = 1/12$.

Nonlinear models for LES have also been proposed independently of the similarity model. Lund & Novikov (1992) have performed a priori analysis of DNS by using a spectral cutoff filter, examining all tensorially allowed nonlinear combinations of filtered velocity gradients. They have found only weak improvements in measures of local agreement between real and modeled stresses (such as correlation coefficients) as the number of terms is increased. However, in a posteriori tests (see also Section 5.3), the addition of nonlinear or similarity terms has proven beneficial. For instance, Kosović (1997) has proposed a model of the form $\tau_{ij}^{\Delta,\rm nl} = -2\nu_T\tilde{S}_{ij} + c_1\Delta^2\tilde{S}_{ik}\tilde{S}_{kj} + c_2\Delta^2(\tilde{R}_{ik}\tilde{S}_{kj} + \tilde{R}_{jk}\tilde{S}_{ki})$, where R_{ij} is the antisymmetric part of the filtered velocity gradient. This model would be equivalent to the mixed nonlinear model if it includes a term $c_3\tilde{R}_{ik}\tilde{R}_{kj}$ and if $c_1 = c_2 = c_3$. Applications of the model to LES of the atmospheric boundary layer show significant improvements over use of only the eddy viscosity part.

5.2 Effects of Spectral Overlap on Correlation

The similarity model has been justified in part by the high correlation between $\boldsymbol{\tau}^{\Delta,\rm sim}$ and $\boldsymbol{\tau}^{\Delta}$. However, the correlation decreases to almost zero when a spectral cutoff filter is used. This behavior raises the possibility that the high correlation observed with other filters could be caused by the use of common information for computing both the real and modeled stresses. On the other hand, a low correlation with a spectral filter may be caused by its inherent oscillatory and nonlocal impact in physical space. This effect can cause scrambling of the spatial relationship between $\boldsymbol{\tau}^{\Delta}$ and $\boldsymbol{\tau}^{\Delta,\rm sim}$. Hence, comparison requires separating between large and small scales by using a projection (see Section 2.2), but without the adverse effects of the cutoff filter. To achieve this goal by using the spatially local box filter, one can sample $\tilde{\mathbf{u}}$ on a discrete lattice of mesh-size Δ (Liu et al 1994, Schumann 1975) and evaluate $\tau_{ij}^{\Delta,\rm sim}$ only from the discrete data. The resulting correlation typically decreases, but to a still appreciable 60% (Liu et al 1994). In contrast, a test field with random phases and amplitudes that follow a $-5/3$ energy spectrum yields a correlation of only $\sim$30%. Thus not all of the elevated correlation is from a trivial use of the same information in the resolved and SGS ranges.

5.3 Comparative A Posteriori Studies

Detailed and careful a posteriori studies of various models have begun to appear in recent years. Vreman et al (1997) present comprehensive results in LES of a temporally developing mixing layer. As shown in Table 1, they compare a number of models by using an extensive list of diagnostic variables ranging from the time

TABLE 1 Comparison of model performance in LES of mixing layer (adapted from Vreman et al 1997, table 2).[a]

Diagnostic variable	M1	M2	M3	M4	M5	M6
Total kinetic energy $\left[\int \frac{1}{2}\,\rho\tilde{u}_i\tilde{u}_i\; d^3\mathbf{x}\right]$	−	+	−	0	+ +	+
SGS dissipation $\left[\int\; -\;(\rho\tau^{\Delta}_{ij}\tilde{S}_{ij})\; d^3\mathbf{x}\right]$	−	+	−	+ +	+	+
Backscatter $\left[\int \min(-\rho\tau^{\Delta}_{ij}\tilde{S}_{ij},\, 0)\; d^3\mathbf{x}\right]$	−	0	−	−	0	0
Stress magnitude [L_2 norm of τ^{Δ}_{12}]	−	+	0	−	+	+
Energy spectrum $E(k_1)$	−	−	−	+	+ +	0
Vorticity in a plane $[\tilde{\omega}_3(x_1, x_2)]$	−	−	−	+	+ +	+
Maximum vorticity	−	−	−	+	+	0
Momentum thickness	−	+	−	−	+	+ +
$\langle\tilde{u}'_1\tilde{u}'_1\rangle$	−	+	−	+	+	+ +
$-\langle\tilde{u}'_1\tilde{u}'_2\rangle$	−	−	−	0	+ +	+

[a]The symbols −, 0, and + refer to bad, reasonable, and good results, respectively. + + is better than +. M1 = constant coefficient Smagorinsky model; M2 = pure similarity model with $C_{\text{sim}} = 1$ and $\gamma = 1$ without eddy viscosity; M3 = nonlinear model with $C_{\text{n1}} = 1/12$, without eddy viscosity but with a clipping procedure to avoid backscatter; M4 = dynamic Smagorinsky; M5 = dynamic mixed model with $\gamma = 1$ and $C_{\text{sim}} = 1$; M6 = dynamic mixed nonlinear model, with $C_{\text{n1}} = 1/12$. Dynamic models use averaging over the homogeneous direction ($x_1 - x_3$ planes).

evolution of total kinetic energy, SGS dissipation, to momentum thickness evolution and rms values. A comparison of their filtered DNS with the LES predictions clearly shows that the mixed dynamic models yield improved results over the pure Smagorinsky or pure similarity models. Also, use of the dynamic procedure improves the Smagorinsky model.

Another detailed comparison of various models is described in Sarghini et al 1999. Two flows are considered: fully developed planar channel flow at two Reynolds numbers and a three-dimensional nonequilibrium flow consisting of a plane channel flow with impulsively started spanwise motion of the walls. Sarghini et al compare the standard and dynamic Smagorinsky models with wall-parallel and Lagrangian averaging, as well as dynamic mixed models with Lagrangian averaging. The comparison is based on profiles of mean velocity, resolved Reynolds stress, SGS kinetic energy, and SGS dissipation. The results show that use of the dynamic procedure, Lagrangian averaging, and adding a similarity term improves the predictions. Also, Sarghini et al find that the similarity term contributes about half of the SGS dissipation. Results with a full two-parameter dynamic model, in which both c_s and C_{sim} are obtained dynamically with Lagrangian averaging (Anderson & Meneveau 1999), are found to be less accurate, especially at high Reynolds numbers. Sarghini et al (1999) point out that this model requires filtering at 4Δ, which exceeds the local integral scale and

invalidates the scale-invariance assumption near a wall (see also Cook 1997). In terms of computing costs, Sarghini et al find that even the relatively complicated, two-parameter, dynamic Lagrangian model increases CPU times by only 30% over the traditional Smagorinsky model. It appears safe to say that the improvements from better SGS models are more significant than the results that could possibly be achieved with an improved spatial resolution at a similar CPU cost (in this case only about 7% finer spatial resolution in each direction, because $1.30^{1/4} \sim 1.067$).

Another version of the dynamic mixed model has been proposed and tested in Horiuti (1997). It is based on the Leonard decomposition of the SGS stress into Reynolds, cross, and Leonard stresses (Leonard 1974, Germano 1986). Each term is modeled separately by using the scale similarity concept. The conclusions are generally consistent with Vreman et al (1997) in that the addition of a similarity term improves the results. As in Sarghini et al (1999), difficulties arise for some versions of the model when the dynamic procedure is applied to solve for two coefficients, especially at coarse resolutions. Akhavan et al (1999) consider a mixed dynamic model with $\gamma = 4/3$, $C_{\text{sim}} = 1$, implemented with a cut-off filter. The dynamic Smagorinsky coefficient is determined without any averaging. Consequently, negative viscosities arise, which must be clipped to zero for numerical stability. Simulations in channel and planar jet flow confirm that the addition of a similarity term yields improved predictions.

Finite-volume simulations of isotropic turbulence have been performed by Fureby et al (1997). They consider a dynamic eddy viscosity model, a one-equation model, and a nondynamic mixed model (with $\gamma = 1$ and $C_{\text{sim}} = 1$). They notice advantages of adding an equation for kinetic energy to account for memory effects, but notice little effect from the similarity term, except for a small degradation of the results at coarse resolutions. Anderson & Meneveau (1999) find that the similarity term has strong effect on the SGS force in finite-volume simulations of forced and decaying isotropic turbulence. They also find that the dynamic similarity (and nonlinear) coefficient is more susceptible to yielding inaccurate results than the dynamic Smagorinsky model at coarse resolutions (when $\Delta \to \ell$). Winckelmans et al (1998) perform spectral LES of decaying isotropic turbulence (with a Gaussian filter, $\gamma = 1$, and $C_{\text{nl}} = 1/12$) and find a positive impact of the similarity term on the decay rate of energy and enstrophy.

In concluding this chapter, one is left still wondering about the dynamical reasons for the overall improvements that result from including the similarity model in LES. One suspects that there are reasons beyond the higher correlation coefficients observed in a priori tests, whose status as a determining figure of merit is still open to debate. Maybe the mixed model simply provides more flexibility with an additional term that is statistically (nearly) orthogonal to the strain-rate tensor (similar to τ_{ij}^{Δ}, the tensor $\tau_{ij}^{\Delta,\text{sim}}$ is poorly correlated with $\tilde{S}_{ij}$). In this way, one is able to reproduce not only mean energy dissipation, but also some other mean quantity such as the mean SGS stress. Or maybe improvements are

caused by the fact that, like the real SGS stress, the similarity model is second order in velocities. Or, as argued in Liu et al (1994), if one were to solve a dynamical equation for scales smaller than Δ (say in a band between $\Delta/2$ and Δ), the additional equation resembles the equation that governs the evolution of the scales in band Δ to 2Δ that are already being simulated in LES. An argument often made [e.g. Akhavan et al (1999), Sarghini et al (1999)] is that the eddy viscosity term models distant interactions, that is, among scales below Δ and much larger than Δ, whereas the similarity term models the local interactions, that is, among scales below Δ and marginally larger than Δ.

6. TESTING SGS MODELS, CONTINUED

This section resumes the discussion of Section 2 about various methods of comparing modeled and real SGS stresses. As discussed in Section 2.3, many such comparisons have been based on correlation coefficients. Adrian (1990) proposes instead to consider how models minimize the square error of the SGS stress divergence $\mathscr{E}_{\nabla\cdot\tau} \equiv \langle(\nabla \cdot \boldsymbol{\tau}^{\Delta} - \nabla\cdot\boldsymbol{\tau}^{\Delta,\mathrm{mod}})^2\rangle$. Minimizing $\mathscr{E}_{\nabla\cdot\tau}$ implies minimizing the mean square error in the prediction of $\partial\tilde{\mathbf{u}}/\partial t$ (Equation 2). Thus, it suggests a best possible prediction for the short-time future evolution of the system. Although the square error and correlation coefficient between two random variables are simply related [both being second-order moments of their joint distribution (Liu et al 1999)], the square error provides a more stringent test. If the correlation coefficient is low, the square error is large, but not vice-versa because even highly correlated variables can have substantially different mean values and/or variances. For the Smagorinsky model, errors as large as 0.97 out of a maximum of 1 without a model have been measured (Liu et al 1999). The similarity model yields smaller errors, of $\sim$0.6.

Optimal estimation theory shows that the predictor (model) that produces the smallest square error for given available data is equal to the conditional average of the variable, conditioned on the available data (Adrian 1990, Langford & Moser 1999). It shows that an optimal LES model that does not include memory effects is given by the multipoint conditional average $\mathfrak{g}_i(\tilde{\mathbf{V}}_1, \tilde{\mathbf{V}}_2, \ldots \tilde{\mathbf{V}}_N \ldots) \equiv \langle\partial_j\tau_{ij} \mid \tilde{\mathbf{V}}_1, \tilde{\mathbf{V}}_2, \ldots \tilde{\mathbf{V}}_N \ldots\rangle$ where $\tilde{\mathbf{V}}_1, \tilde{\mathbf{V}}_2, \ldots \tilde{\mathbf{V}}_N \ldots$ are velocities at all points of the flow. Other efforts at formulating SGS models by using optimization concepts are described in Berkooz (1993) and Chorin et al (1998).

The foregoing arguments are motivated by the desire that a model reproduce the SGS stress so that the LES predicts the correct flow evolution. As has been pointed out repeatedly (e.g. Meneveau 1994, Machiels 1997, Langford & Moser 1999), chaotic systems such as the LES equations inherently preclude long-time predictability. Thus, individual flow realizations produced by LES are not expected to match with real data after some time. To date only a few studies of the decorrelation properties of SGS models have been reported (Shtilman & Chas-

nov 1992, Dubois et al 1997). The subject is closely related to the problem of inverse error-cascade (see Lesieur 1997, Chapter XI).

However, as discussed in Section 2.3, a reasonable expectation is for the model to reproduce mean values, e.g. the correct $\langle \tilde{\mathbf{u}} \rangle$. The ensemble average of Equation 2 shows that, for LES to reproduce the correct $\langle \tilde{\mathbf{u}} \rangle$ and second-order resolved moments, one must at least enforce that $\nabla \cdot \langle \boldsymbol{\tau}^{\Delta,\mathrm{mod}} \rangle = \nabla \cdot \langle \boldsymbol{\tau}^{\Delta} \rangle$ (or $\langle \boldsymbol{\tau}^{\Delta,\mathrm{mod}} \rangle = \langle \boldsymbol{\tau}^{\Delta} \rangle + \mathbf{C}$, where $\mathbf{C}$ is an arbitrary divergence-free tensor field). This condition is necessary and also important for mean momentum transport when $\Delta \to \ell$. But it is not a sufficient condition to guarantee correct predictions because, even if it holds, the LES could lead to erroneous second-order moments, $\langle \tilde{u}_i' \tilde{u}_j' \rangle$, and thus to the wrong mean velocity field (Meneveau 1994). Next, the equation for second-order moments $\langle \tilde{u}_i \tilde{u}_j \rangle$ includes the SGS dissipation tensor $P_{ij}^{\Delta} = -\langle \tau_{ik}^{\Delta} \tilde{S}_{kj} + \tau_{jk}^{\Delta} \tilde{S}_{ki} \rangle$, which should be correctly reproduced by a model. Even this requirement is not a sufficient condition, because third-order moments and pressure-strain correlations also appear in the equation for resolved Reynolds stresses. Continuing to higher orders gives an unclosed hierarchy of necessary, but not sufficient conditions (Meneveau 1994).

One exception in which a sufficient condition exists (Meneveau 1994) is based on the von Karman-Howarth-Kolmogorov (KHK) equation written for structure functions of the filtered velocity in high-Reynolds-number, locally isotropic turbulence. The equation shows that it is sufficient that the two-point stress-velocity correlation $\langle u_1(\mathbf{x} + r\mathbf{e}_1)\, \tau_{11}^{\Delta}(\mathbf{x}) \rangle$ is correctly predicted by a model, to reproduce the correct resolved third-order structure function $\langle [\tilde{u}_1(\mathbf{x} + r\mathbf{e}_1) - \tilde{u}_1(\mathbf{x})]^3 \rangle$. In Fourier space, the KHK equation for the filtered velocity shows that, if the SGS dissipation spectrum is correctly predicted, the correct resolved transfer spectrum results. The latter implies that energy is being transferred at the correct rate among resolved modes, towards the SGS range.

In an interesting development, Langford & Moser (1999) and Pope (2000) show that the hierarchy of necessary conditions is closed for the multipoint probability density function. It turns out that it is sufficient to reproduce the correct multipoint conditional average $\mathfrak{g}_i(\tilde{\mathbf{V}}_1, \tilde{\mathbf{V}}_2, \ldots \tilde{\mathbf{V}}_N \ldots)$ to reproduce all statistics of the resolved field. Analysis of DNS data in isotropic turbulence (Langford & Moser 1999) using a spectral-cutoff filter shows that even the optimal predictor $\mathfrak{g}_i$ (its approximation by several stochastic estimators) leaves the square error very large and that the nonrandom, predictable part of the SGS stress accounts only for spectral energy dissipation.

These considerations underscore the special status and importance of SGS dissipation Π^{Δ} in LES and in a priori tests, especially in isotropic turbulence. However, for general flows it remains necessary to also consider other criteria to evaluate SGS models. Ideally one should consider the full multipoint conditional average $\mathfrak{g}_i$, but it remains a prohibitively difficult quantity to measure. Progress can still be made by considering conditional averages based on a finite number of points. Such conditional averages can be used to isolate specific flow conditions, such as coherent structures (see below).

7. COHERENT STRUCTURES, NONEQUILIBRIUM, AND INTERMITTENCY

One of the promises of LES as compared with RANS is that it can capture unsteady large-scale coherent structures. Indeed, coherent structures have been repeatedly observed in LES of engineering (e.g. Lesieur & Métais 1996) and environmental (Lin et al 1996, Khanna & Brasseur 1998) flows. An important question that so far has received little attention is how the SGS stress and models affect the coherent structures. As shown in Vreman et al (1997), different models lead to qualitative differences in the coherent structures of a mixing layer. Of the models considered, the mixed dynamic model appears to lead to results closest to those of the filtered DNS.

In a priori studies of the DNS of channel flow, Piomelli et al (1996) have used conditional averaging to identify coherent structures associated with forward- and reverse-cascade regions near the wall. The similarity model is found to reproduce the conditional flow structure better than the Smagorinsky model. Hot-wire data in a cylinder wake (O'Neil & Meneveau 1997) have been used to measure a one-dimensional surrogate of the SGS energy dissipation $-\tau_{11}^{\Delta}\tilde{S}_{11}$. Phase averaging with respect to the spanwise von Karman roller vortices shows that they have a strong impact on the spatial distribution of the dissipation, even at filter scales much smaller than those of the large-scale vortices (Δ is well inside the inertial range). Both the dynamic Smagorinsky (with a conditionally averaged coefficient) and the similarity models are able to capture this trend; however, the constant-coefficient Smagorinsky model gives a much more unrealistic distribution of dissipation. Conditional averaging of atmospheric-boundary-layer data similarly has shown that strong up- or down-draft events (identified by large temperature jumps) strongly affect details of the SGS structure (Porté-Agel et al 1998a, 1999). Conditional averaging of PIV data (Meneveau & Katz 1999b) also shows that the mixed-similarity model performs well in reproducing the conditional SGS dissipation rate yielding better results than either the Smagorinsky or similarity models alone. The measurements reported in that paper also quantify the effects of SGS force on the resolved pressure field and its relationship to high strain-rate and energy cascade regions.

The instabilities and rollup of vortices as separated boundary layers transition into turbulent shear layers pose special challenges for SGS modeling. Initially, small-scale vortices within the shear layer interact to create substantially larger structures. This rollup is then followed by pairing of vortices to form even larger eddies. Thus, the shear layer growth includes a reverse-cascading process, and, indeed, using PIV of flow within pumps, Sinha et al (1999 submitted) show that Π^{Δ} is consistently negative near a separating boundary layer region. Ideally, Δ should be small enough to allow capturing such processes in LES without having to rely on the SGS model. In practice, however, such resolutions are often prohibitive, and the shear layers cannot be fully resolved. This case is extremely challenging for an SGS model. It is already well established (Hussain 1986) that

the boundary layer structure has substantial impact on the wavelength of the rolled-up vortices. As extreme examples, several studies (Bell & Mehta 1993, Browand & Latigo 1979, Gopalan et al 1999) have demonstrated that the near-field velocity fluctuations can be three- to sixfold higher when the separating boundary layer is laminar, compared with those fluctuations of a turbulent boundary layer. Gopalan et al (1999) also show that, in the high-Reynolds-number laminar case, the rollup of spanwise eddies is preceded by formation of powerful three-dimensional structures. Another phenomenon is the formation and straining of axial secondary eddies in the braids between the primary vortices (Bernal & Roshko 1986). The straining process may shrink the secondary structures into the subgrid range. If not properly captured by a model, in an LES this effect would result in vortices with the wrong size. This process also represents direct impact of large structures on the dynamics of eddies with significantly smaller sizes.

Efforts have also been devoted to examining directly the effects of rapid distortion (of homogeneous turbulence) on the SGS stress and its models. Early on, McMillan et al (1980) have used DNS of isotropic turbulence at low R_λ ($\sim$40) to study (a priori) the response of the Smagorinsky coefficient and correlation coefficients to plane strain. More recently, Piomelli et al (1997) examine the Smagorinsky, dynamic Smagorinsky, and similarity models in DNS of channel flow undergoing rapid streamwise acceleration and sudden lateral motion of the wall. The dynamic and mixed models are found to reproduce realistically the response of SGS dissipation. Rapid axisymmetric expansion has been studied experimentally in a water tank facility by using cinematic planar PIV (Liu et al 1999). The Smagorinsky model with a constant coefficient, determined from isotropic turbulence data, underpredicts the dissipation during rapid straining. The cause for this effect can be traced to the direct (or rapid) impact of the mean distortion on the SGS stress. A similar direct effect has been reported recently in the analysis of DNS of rapidly distorted turbulence (Shao et al 1999). The similarity model with a constant coefficient, on the other hand, overpredicts SGS dissipation (Liu et al 1999). Owing to these opposite trends, the mixed model provides better predictions of the SGS dissipation but still underpredicts the SGS stress.

The previous discussion focused mainly on the effects of large-scale coherent structures. But coherent structures also occur at the smallest scales, near η in DNS. Specifically, the tubular structure of high-vorticity regions [''worms'' (Vincent & Meneguzzi 1991)] has received considerable attention. Interestingly, such structures are also observed in LES near the smallest resolved scales (see Meneveau et al 1996, Fureby et al 1997), although they are thicker of course. The presence of such ''fat worms'' in turbulence has been confirmed from filtered DNS (e.g. see Figure 17 of Vincent & Meneguzzi 1991). Detailed quantitative comparisons of such structures are still lacking. A related feature of small-scale structures is spatial intermittency, usually studied by means of structure functions (e.g. see Sreenivasan & Antonia 1997). Dimensionally, the SGS stress resembles squared velocity differences over a distance Δ (Vreman et al 1994b, Eyink 1996),

and thus $\Pi^{\Delta}(\mathbf{x}, t)$ is dimensionally similar to the third-order structure function $[\tilde{u}_L(\mathbf{x} + r\mathbf{e}_L) - \tilde{u}_L(\mathbf{x})]^3/\Delta$. Indeed, Cerutti & Meneveau (1998) find that scaling exponents of high-order moments of $\Pi^{\Delta}(\mathbf{x}, t)$ compare well with those of longitudinal velocity structure functions. Both sets of exponents clearly depart from the Kolmogorov (1941) theory that disregards inner intermittency.

8. OTHER RECENT SUBGRID SCALE MODELS

A number of new ideas have emerged in the past few years as alternatives to the eddy viscosity and similarity models. They do not postulate a specific form for the stress tensor but, rather, for the subgrid velocity field. The three model classes summarized in this section display the appropriate inertial-range scale invariance properties (in the mean).

Domaradzki & Saiki (1997) propose a model in which an ''estimated SGS velocity field'' is constructed between the scales Δ and $\Delta/2$. In Fourier space, the required additional modes are determined from two conditions: (*a*) a self-consistency condition, that is, that the top-hat–filtered SGS velocity is equal to the grid level velocity at available grid points; and (*b*) the assumption that the phase of the SGS modes is equal to the phase of the nonlinear terms of the resolved velocity field. A priori tests based on DNS of channel flow and comparisons with the Smagorinsky model show improved correlation coefficients between stresses ($\sim$0.5). Interestingly, in a posteriori tests this model was found to be sufficiently dissipative without an additional eddy viscosity term.

Efforts at generating broad-band synthetic velocity fields that extend down to the Kolmogorov scale include the linear-eddy model of Kerstein (1988) and several fractal models (e.g. see Juneja et al 1994, Benzi et al 1993). For applications to LES, the model of Scotti & Meneveau (1997) uses fractal interpolation. A local mapping is constructed that transforms features of the $\tilde{\mathbf{u}}$ signal, at scales even coarser than Δ, onto the complete (known) signal $\tilde{\mathbf{u}}$. Iteration of this mapping generates a fractal, scale-invariant signal. This technique allows the computation of integrals of any power of the full signal, allowing analytical evaluation of the SGS stress without explicit construction of the fractal SGS field. Applications to LES of the one-dimensional Burgers equation and the three-dimensional filtered Navier-Stokes equations (Scotti & Meneveau 1997, 1999) show that the assumption of fractality (or scale invariance) alone is not enough to produce good results, owing to insufficient SGS dissipation. In one dimension, this problem can be solved with an additional transport equation to dynamically determine the local fractal dimension and SGS kinetic energy. This option is prohibitively complicated in three dimensions. A workable extension to three dimensions uses prescribed fractal dimensions in different eigendirections of the resolved strain rate tensor, which leads to good results in forced and decaying isotropic turbulence.

Based on the work of Pullin & Saffman (1993), Misra & Pullin (1997) propose to represent the SGS turbulence as stretched vortices, which are local solutions

to the Navier-Stokes equations. The SGS stresses are computed analytically from the implied local velocity field and depend on the SGS kinetic energy and orientation of the SGS vortices. A relationship between the orientation of vortices and the resolved field must be postulated. Several options, such as aligning the SGS vortices with the largest positive eigendirection of $\tilde{S}_{ij}$ or allowing a fraction of them to be aligned with the resolved vorticity, have been explored. Tests in forced and decaying isotropic turbulence (Misra & Pullin 1997) yield promising results.

9. CONCLUSIONS

In this review we have described several SGS models, including the traditional Smagorinsky model and two model classes that explicitly use the scale invariance properties of high-Reynolds-number turbulence: the dynamic- and the mixed-similarity models. A growing body of literature has been reviewed to exhibit their strengths and weaknesses. Reflecting the inherent complexity of the SGS closure problem, there are a number of different criteria for comparing real and modeled stresses, but few universally agreed upon procedures. It is still premature to venture a final verdict as to which of the existing models is best for LES. Nonetheless, a priori tests in a variety of flow conditions show that mixed models are, on the whole, superior to pure eddy viscosity models. Coefficients obtained dynamically have also led to improved predictions. To date there are relatively few a posteriori comparisons of a meaningful variety of models with a consistent set of flow conditions and numerical methods. However, the available references reach the same conclusions, namely that the dynamic procedure improves the Smagorinsky model and that the addition of a similarity term leads to more accurate results in LES. Hence, it can be concluded that the use of scale invariance concepts in SGS modeling has proven beneficial.

Returning to Richardson's rhyme quoted in Section 1, advocacy of scale invariance-based turbulence models inspires the following variation:

> *"LES whorls have subgrid whorls,*
> *which feed on their velocity,*
> *but small whorls copy larger whorls,*
> *so we don't need viscosity*
> *(in the molecular sense).*"

Such a pronouncement is too optimistic. As has been outlined in this article, there are indications of direct effects of very large-scale events on small-scale features, of scale dependence in model coefficients, of complex effects of rapid distortion, etc. Such observations suggest that realistic models will have to tackle deviations from scale invariance explicitly, especially when dealing with turbulence outside or near the limits of the inertial range. Nevertheless, scale invariance symmetry in the inertial range is still a useful constraint, at least as a starting

point for more refined lines of attack. It may be instructive to recall that, in renormalization group techniques (e.g. see McComb 1990), scale invariance arises as a baseline from which deviations are captured by perturbation methods. SGS modeling with dynamic and/or similarity models may therefore lead to developments of RNG-like tools that better integrate turbulence theory and simulation. Furthermore, the study and continued development of SGS models require high-Reynolds-number data and therefore a greater integration of experimental with numerical and theoretical research in turbulence.

ACKNOWLEDGMENTS

We thank U. Piomelli, T. S. Lund, O. M. Knio, S. B. Pope, and B. Geurts for reading the manuscript and for their valuable suggestions. The contributions of students and collaborators identified in the cited literature were invaluable in giving content to this article. We gratefully acknowledge the sustained financial support from the National Science Foundation and the Office of Naval Research (P. Purtell, program manager). CM also thanks the Center for Turbulence Research (Stanford/NASA Ames) for the hospitality during various summer programs. S. Chester's help with the bibliography is much appreciated.

LITERATURE CITED

Adrian RJ. 1990. Stochastic estimation of subgrid scale motions. *Appl. Mech. Rev.* 43:S214–S218

Akhavan R, Ansari A, Kang S, Mangiavacchi N. 1999. Subgrid-scale interactions in a numerically simulated planar turbulent jet and implications for modeling. *J. Fluid Mech.* Submitted

Akselvoll K, Moin P. 1996. Large-eddy simulation of turbulent confined coannular jets. *J. Fluid Mech.* 315:387–411

Anderson R, Meneveau C. 1999. Effects of the similarity model in finite-difference LES of isotropic turbulence using a Lagrangian dynamic mixed model. *Flow, Turbu. & Comb.* 62:201–225

Balaras E, Benocci C, Piomelli U. 1995. Finite-difference computations of high Reynolds-number flows using the dynamic subgrid-scale model. *Theor. Comp. Fluid Dyn.* 7:207–16

Balaras E, Benocci C, Piomelli U. 1996. Two-layer approximate boundary conditions for large-eddy simulations. *AIAA J.* 34:1111–19

Bardina J, Ferziger JH, Reynolds WC. 1980. Improved subgrid scale models for large-eddy simulation. *Am. Inst. Aeronaut. Astronaut. Pap. 80-1357*

Barnhart DH, Adrian RJ, Papen GC. 1994. Phase-conjugate holographic system for high-resolution PIV. *Appl. Opt.* 33:7159–7170

Bastiaans RJM, Rindt CCM, Van Steenhoven AA. 1998. Experimental analysis of a confined transitional plume with respect to subgrid-scale modelling. *Int. J. Heat Mass Trans.* 41:3989–4007

Bell JH, Mehta RD. 1993. Effect of imposed spanwise perturbations on plane mixing-layer structure. *J. Fluid Mech.* 257:33–63

Benzi R, Ciliberto S, Tripiccione R, Baudet C, Massaioli F, Succi S. 1993. Extended self-

similarity in turbulent flows. *Phys. Rev. E* 48:R29–32

Berkooz G. 1993. An observation on probability density equations, or, when do simulations reproduce statistics. *Nonlinearity* 7:313–28

Berkooz G, Holmes P, Lumley JL. 1993. The proper orthogonal decomposition in the analysis of turbulent flows. *Annu. Rev. Fluid Mech.* 25:539–75

Bernal LP, Roshko A. 1986. Streamwise vortex structure in plane mixing layers. *J. Fluid Mech.*, 170:499–525

Borue V, Orszag S. 1998. Local energy flux and subgrid-scale statistics in three-dimensional turbulence. *J. Fluid Mech.* 366:1–31

Browand FK, Latigo BO. 1979. Growth of the two dimensional mixing layer from a turbulent and non-turbulent boundary layer. *Phys. Fluids* 22:1011–19

Canuto VM, Cheng Y. 1997. Determination of the Smagorinsky-Lilly constant c_s. *Phys. Fluids* 7:1368–78

Carati D, Wray A, Cabot W. 1996. Ensemble averaged dynamic modeling. In *Proc. Summer Program, 1994, Cent. Turbul. Res., Stanford Univ., CA* V:237–48

Carati D, Ghosal S, Moin P. 1995a. On the representation of backscatter in dynamic localization models. *Phys. Fluids* 7:606–16

Carati D, Jansen K, Lund TS. 1995b. A family of dynamic models for large-eddy simulation. *Ann. Res. Briefs, Cent. Turbul. Res., NASA Ames/Stanford, CA*, pp. 35–40

Cerutti S, Meneveau C. 1998. Intermittency and relative scaling of subgrid-scale energy dissipation in isotropic turbulence. *Phys. Fluids* 10:928–37

Cerutti S, Meneveau C. 1999. Hot-wire array for turbulence research in subgrid-scale modeling. In *Proc. Am. Soc. Mech. Eng. Fluids Eng.*, FEDSM99-7349

Chasnov JR. 1991. Simulation of the Kolmogorov inertial subrange using an improved subgrid model. *Phys. Fluids A* 3:188–200

Chollet J-P, Lesieur M. 1981. Parametrization of small scales of three-dimensional isotropic turbulence utilizing spectral closures. *J. Atmos. Sci.* 38:2747–57

Chorin AJ, Kast AP, Kupferman R. 1998. Optimal prediction of underresolved dynamics. *Proc. Natl. Acad. Sci. USA* 95:4094–98

Clark RA, Ferziger JH, Reynolds WC. 1979. Evaluation of subgrid–scale models using an accurately simulated turbulent flow. *J. Fluid Mech.* 91:1–16

Colucci PJ, Jaberi FA, Givi P, Pope SB. 1998. Filtered density function for large eddy simulation of turbulent reacting flows. *Phys. Fluids* 10:499–515

Cook AW. 1997. Determination of the constant coefficient in scale similarity models of turbulence. *Phys. Fluids* 9:1485–87

Cook AW, Riley JJ. 1994. A subgrid model for equilibrium chemistry in turbulent flows. *Phys. Fluids* 6:2868–70

Dahm WJA, Southerland KB, Buch KA. 1991. Direct, high-resolution, four-dimensional measurements of the fine scale structure of $Sc \gg 1$ molecular mixing in turbulent flows. *Phys. Fluids A* 3:1115–1127

Dantinne G, Jeanmart H, Winckelmans GS, Legat V. 1998. Hyperviscosity and vorticity-based models for subgrid scale modeling. *Appl. Sci. Res.* 59:409–20

Deardorff JW. 1974. Three-dimensional numerical study of the height and mean structure of a heated planetary boundary layer. *Bound. Layer Meteor.* 7:81

DesJardin PE, Frankel SH. 1998. Large eddy simulation of a nonpremixed reacting jet: Application and assessment of subgrid-scale combustion models. *Phys. Fluids* 10:2298–314

Domaradzki JA, Liu W, Brachet ME. 1993. An analysis of subgrid-scale interactions in numerically simulated isotropic turbulence. *Phys. Fluids A* 5:1747–59

Domaradzki JA, Metcalfe RW, Rogallo RS, Riley JJ. 1987. Analysis of subgrid-scale eddy viscosity with use of results from direct numerical simulations. *Phys. Rev. Lett.* 58:547–50

Domaradzki JA, Saiki EM. 1997. A subgrid-scale model based on the estimation of

unresolved scales of turbulence. *Phys. Fluids* 9:1–17

Dubois T, Jauberteau F, Zhou Y. 1997. Influences of subgrid scale dynamics on resolvable scale statistics in large-eddy simulations. *Physica D* 100:390–96

Erlebacher G, Hussaini MY, Speziale CG, Zang TA. 1992. Toward the large-eddy simulation of compressible turbulent flows. *J. Fluid Mech.* 238:155–85

Eyink GL. 1996. The multifractal model of turbulence and a priori estimates in LES, I and II. *Cent. for Nonlinear Studies Archive*, 9602018, 9602019, Los Alamos, NM

Farge M, Schneider K, Kevlahan N. 1999. Non-Gaussianity and coherent vortex simulations for two-dimensional turbulence using an adaptive orthogonal wavelet basis. *Phys. Fluids* 11:2187–201

Frisch U. 1995. *Turbulence, the legacy of A. N. Kolmogorov.* Cambridge, UK: Cambridge Univ. Press

Fureby C, Tabor G, Weller HG, Gosman AD. 1997. A comparative study of subgrid-scale models in homogeneous isotropic turbulence. *Phys. Fluids* 9:1416–29

Gao F, O'Brien EE. 1993. A large-eddy-simulation scheme for turbulent reacting flows. *Phys. Fluids A* 5:1282–84

Germano M. 1986. A proposal for a redefinition of the turbulent stresses in the filtered Navier-Stokes equations. *Phys. Fluids* 29:2323–24

Germano M. 1992. Turbulence: the filtering approach. *J. Fluid Mech.* 238:325–36

Germano M, Piomelli U, Moin P, Cabot WH. 1991. A dynamic subgrid-scale eddy viscosity model. *Phys. Fluids A* 3:1760–65

Ghosal S. 1996. An analysis of numerical errors in large-eddy simulations of turbulence. *J. Comp. Phys.* 125:187–206

Ghosal S, Lund TS, Moin P, Akselvoll K. 1995. A dynamic localization model for large eddy simulation of turbulent flows. *J. Fluid Mech.* 286:229–55

Ghosal S, Moin P. 1995. The basic equations for the large eddy simulation of turbulent flows in complex geometry. *J. Comp. Phys.* 118:24–37

Ghosal S, Rogers MM. 1997. A numerical study of self-similarity in a turbulent plane wake using large-eddy simulation. *Phys. Fluids* 9:1729–39

Gopalan S, Katz J, Knio OM. 1999. The flow structure in the near field of jets and its effect on cavitation inception. *J. Fluid Mech.* In press

Härtel C, Kleiser L, Unger F, Friedrich R. 1994. Subgrid-scale energy transfer in the near-wall region of turbulent flows. *Phys. Fluids* 6:3130–43

Haworth DC, Jansen K. 1999. LES on unstructured deforming meshes: towards reciprocating IC engines. *Comput. Fluids* In press

Horiuti K. 1997. A new dynamic two-parameter mixed model for large-eddy simulation. *Phys. Fluids* 9:3443–64

Hussain AKMF. 1986. Coherent structures and turbulence. *J. Fluid Mech.* 173:303–56

Im HG, Lund TS, Ferziger JH. 1997. Large eddy simulation of turbulent front propagation with dynamic subgrid models. *Phys. Fluids* 9:3826–33

Jaberi FA, James S. 1998. A dynamic similarity model for large eddy simulation of turbulent combustion. *Phys. Fluids* 10:1775–77

Jordan SA. 1999. A large-eddy simulation methodology in generalized curvilinear coordinates. *J. Comp. Phys.* 148:322–40

Juneja A, Lathrop DP, Sreenivasan KR, Stolovitzky G. 1994. Synthetic turbulence. *Phys. Rev. E* 49:5179–94

Kerstein AR. 1988. A linear-eddy model of turbulent scalar transport and mixing. *Combust. Sci. Technol.* 60:391–421

Khanna S, Brasseur JG. 1998. Three-dimensional buoyancy and shear-induced local structure of the atmospheric boundary layer. *J. Atmos. Sci.* 55:710–43

Kolmogorov AN. 1941. The local structure of turbulence in incompressible viscous fluid for very large Reynolds number. *C.R. Acad. Sci.* USSR 30:301

Kosović B. 1997. Subgrid-scale modelling for the large-eddy simulation of high-Reynolds-number boundary layers. *J. Fluid Mech.* 336:151–82

Kraichnan RH. 1976. Eddy viscosity in two and three dimensions. *J. Atmos. Sci.* 33:1521–36

Kravchenko AG, Moin P. 1997. On the effect of numerical errors in large eddy simulations of turbulent flows. *J. Comp. Phys.* 131:310–22

Landau LD, Lifshitz EM. 1980. *Statistical Physics.* New York: Pergamon

Langford J, Moser RD. 1999. Optimal LES formulations for isotropic turbulence. *J. Fluid Mech.* In press

Leith CE. 1990. Stochastic backscatter in a subgrid-scale model: plane shear mixing layer. *Phys. Fluids A* 2:297–99

Leonard A. 1974. Energy cascade in large-eddy simulations of turbulent fluid flows. *Adv. Geophys.* 18:237

Leonard A. 1997. Large-eddy simulation of chaotic convection and beyond. *Am. Inst. Aeronaut. Astronaut. Pap. 97-0204:1–8*

Lesieur M. 1997. *Turbulence in Fluids.* Dordrecht: Kluwer Academic. 3rd ed.

Lesieur M, Métais O. 1996. New trends in large-eddy simulations of turbulence. *Annu. Rev. Fluid Mech.* 28:45–82

Leslie DC, Quarini GL. 1979. The application of turbulence theory to the formulation of subgrid modeling procedures. *J. Fluid Mech.* 91:65–91

Lilly DK. 1967. The representation of small-scale turbulence in numerical simulation experiments. In *Proc. IBM Scientific Computing Symp. Environ. Sci.,* p. 195

Lilly DK. 1992. A proposed modification of the Germano subgrid-scale closure method. *Phys. Fluids A* 4:633–35

Lin C-L, McWilliams JC, Moeng C-H, Sullivan PP. 1996. Coherent structures and dynamics in a neutrally stratified planetary boundary layer flow. *Phys. Fluids* 8:2626–39

Liu S, Katz J, Meneveau C. 1999. Evolution and modeling of subgrid scales during rapid straining of turbulence. *J. Fluid Mech.* 387:281–320

Liu S, Meneveau C, Katz J. 1994. On the properties of similarity subgrid-scale models as deduced from measurements in a turbulent jet. *J. Fluid Mech.* 275:83–119

Liu S, Meneveau C, Katz J. 1995. Experimental study of similarity subgrid-scale models of turbulence in the far-field of a jet. *Appl. Sci. Res.* 54:177–90

Lund TS, Novikov EA. 1992. Parametrization of subgrid-scale stress by the velocity gradient tensor. In *Cent. for Turbulence Res., Annu. Res. Briefs, Stanford Univ.* 1992:27

Lund TS, Kaltenbach H-J. 1995. Experiments with explicit filtering for LES using a finite-difference method. *Cent. for Turbulence Res., Annu. Res. Briefs,* Stanford Univ. 1995:91–105

Lund TS, Wu X, Squires KD. 1998. Generation of turbulent inflow data for spatially-developing boundary layer simulations. *J. Comp. Phys.* 140:233–58

Machiels L. 1997. Predictability of small-scale motion in isotropic fluid turbulence. *Phys. Rev. Lett.* 79:3411–14

Mansfield J, Knio OM, Meneveau C. 1998. A dynamic LES scheme for the vorticity transport equation: formulation and *a-priori* tests. *J. Comp. Phys.* 145:693–730

Mansfield J, Knio OM, Meneveau C. 1999. Dynamic LES of colliding vortex rings using a 3D vortex method. *J. Comp. Phys.* 152:305–45

Mason PJ. 1994. Large-eddy simulation: a critical review of the technique. *QJR Meteorol. Soc.* 120:1

Mason PJ, Thomson DJ. 1992. Stochastic backscatter in large-eddy simulations of boundary layers. *J. Fluid Mech.* 242:51–78

McComb WD. 1990. *The Physics of Fluid Turbulence.* Oxford, UK: Oxford Sci. Publ.

McMillan OJ, Ferziger JH. 1979. Direct testing of subgrid-scale models. *Am. Inst. Aeronaut. Astronaut. J.* 17:1340–46

McMillan OJ, Ferzinger JH, Rogallo RS. 1980. Tests of new subgrid scale models in

strained turbulence. *Am. Inst. Aeronaut. Astronaut. Pap. 801339*

Meneveau C. 1991. Analysis of turbulence in the orthonormal wavelet representation. *J. Fluid Mech.* 232:469–520

Meneveau C. 1994. Statistics of turbulence subgrid-scale stresses: Necessary conditions and experimental tests. *Phys. Fluids A* 6:815–33

Meneveau C, Katz J. 1999a. Dynamic testing of subgrid models in LES based on the Germano identity. *Phys. Fluids* 11:245–47

Meneveau C, Katz J. 1999b. Conditional subgrid force and dissipation in locally isotropic and rapidly strained turbulence. *Phys. Fluids.* 11:2317–29

Meneveau C, Lund TS, Cabot WH. 1996. A Lagrangian dynamic subgrid-scale model of turbulence. *J. Fluid Mech.* 319:353–85

Meneveau C, Lund TS. 1997. The dynamic Smagorinsky model and scale-dependent coefficients in the viscous range of turbulence. *Phys. Fluids* 9:3932–34

Meneveau C, O'Neil J. 1994. Scaling laws of the dissipation rate of turbulent subgrid-scale kinetic energy. *Phys. Rev. E* 49:2866–74

Meng H, Hussain F. 1995. Instantaneous flow field in an unstable vortex ring measured by HPIV. *Phys. Fluids* 7:9–11

Menon S, Young PK, Kim WW. 1996. Effect of subgrid models on the computed interscale energy transfer in isotropic turbulence. *Comput. Fluids* 25:165–80

Métais O, Lesieur M. 1992. Spectral large-eddy simulation of isotropic and stably stratified turbulence. *J. Fluid Mech.* 239:157–94

Misra A, Pullin DI. 1997. A vortex-based subgrid stress model for large-eddy simulation. *Phys. Fluids* 9:2443–54

Moeng C-H. 1984. Large-eddy simulation model for the study of planetary boundary-layer turbulence. *J. Atmos. Sci.* 41:2052–62

Moin P, Kim J. 1982. Numerical investigation of turbulent channel flow. *J. Fluid Mech.* 118:341–77

Moin P, Squires KD, Cabot WH, Lee S. 1991. A dynamic subgrid-scale model for compressible turbulence and scalar transport. *Phys. Fluids A* 3:2746–57

Murray JA, Piomelli U, Wallace JM. 1996. Spatial and temporal filtering of experimental data for a-priori studies of subgrid-scale stresses. *Phys. Fluids* 8:1978–80

Najjar FM, Tafti DK. 1996. Study of discrete test filters and finite difference approximations for the dynamic subgrid-scale stress model. *Phys. Fluids* 8:1076–88

O'Neil J, Meneveau C. 1997. Subgrid-scale stresses and their modeling in a turbulent plane wake. *J. Fluid Mech.* 349:253–93

Piomelli U. 1993. High Reynolds number calculations using the dynamic subgrid scale stress model. *Phys. Fluids A* 5:1484–90

Piomelli U, Cabot WH, Moin P, Lee S. 1991. Subgrid-scale backscatter in turbulent and transitional flows. *Phys. Fluids A* 3:1766–71

Piomelli U, Coleman GN, Kim J. 1997. On the effects of nonequilibrium on the subgrid-scale stresses. *Phys. Fluids* 9:2740–48

Piomelli U, Liu J. 1995. Large-eddy simulation of rotating channel flows using a localized dynamic model. *Phys. Fluids* 7:839–48

Piomelli U, Moin P, Ferziger JH. 1988. Model consistency in large eddy simulation of turbulent channel flows. *Phys. Fluids* 31:1884–91

Piomelli U, Yu Y, Adrian RJ. 1996. Subgrid-scale energy and near-wall turbulence structure. *Phys. Fluids* 8:215–24

Piomelli U, Zang TA. 1991. Large-eddy-simulation of transitional channel flow. *Comput. Phys. Commun.* 65:224–30

Pope SB. 1985. Pdf methods for turbulent reactive flows. *Prog. Energy Combust. Sci.* 11:119–92

Pope SB. 1990. Computations of Turbulent combustion: progress and challenges. *23rd Symp. Int. on Combustion. Combustion Inst.*, pp. 519–612

Pope SB. 2000. *Turbulent Flows.* Cambridge, UK: Cambridge Univ. Press

Porté-Agel F, Meneveau C, Parlange MB. 1998a. Some basic properties of the surrogate subgrid-scale heat flux in the atmospheric boundary layer. *Boundary Layer Meteoro.* 88:425–44

Porté-Agel F, Meneveau C, Parlange MB. 1998b. A scale-dependent dynamic model for large-eddy simulation: application to the atmospheric boundary layer. *J. Fluid Mech.* Submitted

Porté-Agel F, Parlange MB, Meneveau C, Eichinger WE, Pahlow M. 1999. Subgrid-scale dissipation in the atmospheric surface layer: Effects of stability and filter dimension. *J. Hydrometeorol.* In press

Pullin DI, Saffman PG. 1993. On the Lundgren-Townsend model of turbulent fine scales. *Phys. Fluids A* 5:126–45

Réveillon J, Vervisch L. 1996. Response of the dynamic LES model to heat release induced effects. *Phys. Fluids* 8:2248–50

Richardson. LF. 1922. *Weather Prediction by Numerical Process.* Cambridge, UK: Cambridge Univ. Press

Rodi W, Ferziger JH, Breuer M, Pourquie M. 1997. Status of large eddy simulation: results of a workshop. *J. Fluids Eng.-T ASME,* 119:248–62

Rogallo RS, Moin P. 1984. Numerical simulation of turbulent flows. *Annu. Rev. Fluid Mech.* 16:99–137

Saddoughi SG, Veeravalli SV. 1994. Local isotropy in turbulent boundary layers at high Reynolds number. *J. Fluid Mech.* 268:333–372

Salvetti MV, Banerjee S. 1995. A-priori tests of a new dynamic subgrid-scale model for finite-difference large-eddy simulations. *Phys. Fluids* 7:2831–47

Sarghini F, Piomelli U, Balaras E. 1999. Scale-similar models for large-eddy simulations. *Phys. Fluids.* 11:1596–607

Schumann U. 1975. Subgrid scale model for finite difference simulations of turbulent flows in plane channels and annuli. *J. Comp. Physics.* 18:376–404

Schumann U. 1995. Stochastic backscatter of turbulence energy and scalar variance by random sub-grid scale fluxes. *Proc. R. Soc. London Ser. A* 451:293–318

Scotti A, Meneveau C. 1997. Fractal model for coarse-grained nonlinear partial differential equations. *Phys. Rev. Lett.* 78:867–70

Scotti A, Meneveau C. 1999. A fractal model for large eddy simulation of turbulent flow. *Physica D.* 127:198–232

Scotti A, Meneveau C, Fatica M. 1997. Dynamic Smagorinsky model on anisotropic grids. *Phys. Fluids* 9:1856–58

Scotti A, Meneveau C, Lilly DK. 1993. Generalized Smagorinsky model for anisotropic grids. *Phys. Fluids A* 5:2306–8

Shao L, Sarkar S, Pantano C. 1999. On the relationship between the mean flow and subgrid stresses in LES of turbulent shear flows. *Phys. Fluids* 11:1229–48

Shaw R, Schumann U. 1992. Large-eddy simulation of turbulent flow above and within a forest. *Boundary Layer Meteoro.* 61: 47–64

Shtilman L, Chasnov JR. 1992. LES vs. DNS: a comparative study. *In Proc. Summer Program, Cent. Turbul. Res., Stanford Univ.,* 3:137

Sinha M, Katz J, Meneveau C. 1999. Quantitative visualization of the flow in a centrifugal pump with diffuser vanes. Part B: Addressing passage-averaged and LES modeling issues in turbomachinery flows. *J. Fluids Eng.* Submitted

Smagorinsky J. 1963. General circulation experiments with the primitive equations. I. The basic experiment. *Mon. Weather Rev.* 91:99

Smith LM, Woodruff SL. 1998. Renormalization-group analysis of turbulence. *Annu. Rev. Fluid Mech.* 30:275–310

Speziale CG. 1985. Galilean invariance of subgrid-scale stress models in LES of turbulence. *J. Fluids Mech.* 156:55–62

Speziale CG. 1991. Analytical methods for the development of Reynolds-stress closures in turbulence. *Annu. Rev. Fluid Mech.* 23:107–157

Sreenivasan KR. 1991. Fractals and multifractals in turbulence. *Annu. Rev. Fluid Mech.* 23:539–600

Sreenivasan KR. 1995. On the universality of the Kolmogorov constant. *Phys. Fluids* 7:2778–84

Sreenivasan KR, Antonia RA. 1997. The phenomenology of small-scale turbulence. *Annu. Rev. Fluid Mech.* 29:435–72

Tao B, Katz J, Meneveau C. 1999. Applications of HPIV data of turbulent duct flow for turbulence modeling, *Proc. Am. Soc. Mech. Eng. Pap. FEDSM99-7281*

Tong C, Wyngaard JC, Khanna S, Brasseur JG. 1998. Resolvable- and subgrid-scale measurements in the atmospheric surface layer: technique and issues. *J. Atmos. Sci.* 55:3114–26

Vincent A, Meneguzzi M. 1991. The spatial structure and statistical properties of homogeneous turbulence. *J. Fluid Mech.* 225:1–20

Voke PR. 1996. Subgrid-scale modeling at low mesh Reynolds number. *Theor. Comp. Fluid Dyn.* 8:131–43

Vreman B, Geurts B, Kuerten H. 1994a. On the formulation of the dynamic mixed subgrid-scale model. *Phys. Fluids* 6:4057–59

Vreman B, Geurts B, Kuerten H. 1994b. Realizability conditions for the turbulent stress tensor in large-eddy simulation. *J. Fluid Mech.* 278:351–62

Vreman B, Geurts B, Kuerten H. 1995. Subgrid-modeling in LES of compressible flow. *Appl. Sci. Res.* 54:191–203

Vreman B, Geurts B, Kuerten H. 1997. Large eddy simulation of the turbulent mixing layer. *J. Fluid Mech.* 339:357–90

Wang Q, Squires KD. 1996. Large eddy simulation of particle-laden turbulent channel flow. *Phys. Fluids* 8:1207–23

Winckelmans GS, Wray AA, Vasilyev OV. 1998. Testing of a new mixed model for LES: the Leonard model supplemented by a dynamic Smagorinsky term. *In Proc. Summer Program VII, Cent. Turbul. Research, Stanford Univ.*

Wu X, Squires KD. 1997. Large eddy simulation of an equilibrium three dimensional turbulent boundary layer. *Am. Inst. Aeronaut. Astronaut. J.* 35:67–74

Wu X, Squires KD. 1998. Numerical investigation of the turbulent boundary layer over a bump. *J. Fluid Mech.* 362:229–71

Yakhot A, Orszag SA, Yakhot Y. 1989. Renormalization group formulation of large-eddy simulations. *J. Sci. Comp.* 4:139

Zang Y, Street RL, Koseff J. 1993. A dynamic mixed subgrid-scale model and its application to turbulent recirculating flows. *Phys. Fluids A* 5:3186–96

Zhang J, Tao B, Katz J. 1997. Turbulent flow measurement in a square duct with hybrid holographic PIV. *Exp. Fluids* 23:373–81

Annual Review of Fluid Mechanics
Volume 32, 2000

CONTENTS